Biogeosciences Discuss., https://doi.org/10.5194/bg-2017-299
Manuscript under review for journal Biogeosciences
Discussion started: 28 July 2017

Biogeosciences Discussions
Open Access
EGU

Mechanisms of dissolved and labile particulate iron supply to shelf waters and phytoplankton blooms off South Georgia, Southern Ocean

Christian Schlosser[1,2,*], Katrin Schmidt[3], Alfred Aquilina[1], William B. Homoky[1,4], Maxi Castrillejo[1,5], Rachel A. Mills[1], Matthew D. Patey[1], Sophie Fielding[3], Angus Atkinson[6], and Eric P. Achterberg[1,2]

[1] Ocean and Earth Science, National Oceanography Centre Southampton, University of Southampton, SO14 3ZH Southampton, United Kingdom
[2] GEOMAR Helmholtz Centre for Ocean Research, Wischhofstr. 1-3, 24148 Kiel, Germany
[3] British Antarctic Survey, CB3 0ET Cambridge, United Kingdom
[4] Department of Earth Sciences, University of Oxford, OX1 3AN Oxford, United Kingdom
[5] Institut de Ciència i Tecnologia Ambientals & Departament de Física, Universitat Autònoma de Barcelona, 08193 Bellaterra, Spain
[6] Plymouth Marine Laboratory, The Hoe, PL1 3DH Plymouth, United Kingdom

* Corresponding author Christian Schlosser (Email: cschlosser@geomar.de, Phone: 0049 (0) 431 600 1297)

Biogeosciences Discuss., https://doi.org/10.5194/bg-2017-299
Manuscript under review for journal Biogeosciences
Discussion started: 28 July 2017

Abstract (349 words)

The island of South Georgia is situated in the iron (Fe) depleted Antarctic Circumpolar Current of the Southern Ocean. Iron emanating from its shelf system fuels large phytoplankton blooms downstream of the island, but the actual supply mechanisms are unclear. To address this we present the first inventory of Fe, manganese (Mn) and aluminium (Al) in shelf sediments, pore waters and the water column in the vicinity of South Georgia, alongside data on zooplankton-mediated Fe cycling processes. The seafloor sediments were the main particulate Fe source to shelf bottom waters as indicated by Fe/Mn and Fe/Al ratios for shelf sediments and suspended particles in the water column. Less than 1% of the total particulate Fe pool was leachable surface adsorbed (labile) Fe, and therefore potentially available to organisms. Pore waters formed the primary dissolved Fe (DFe) source to shelf bottom waters supplying 0.1 – 44 µmol DFe m^{-2} d^{-1}. However, only 0.41 ± 0.26 µmol DFe m^{-2} d^{-1} was transferred to the surface mixed layer by vertical diffusive and advective mixing. Other trace metal sources to surface waters included glacial flour released by melting glaciers and zooplankton excretion processes. On average 6.5 ± 8.2 µmol m^{-2} d^{-1} of labile particulate Fe was supplied to the surface mixed layer via krill faecal pellets, with further DFe released by krill at around 1.1 ± 2.2 µmol m^{-2} d^{-1}. The faecal pellets released by krill constituted of seafloor derived lithogenic material and settled algae debris, in addition to freshly ingested suspended phytoplankton specimen. The phytoplankton Fe requirement in the blooms ca. 1,250 km downstream the island of South Georgia was 0.33 ± 0.11 µmol m^{-2} d^{-1}, with the DFe supply by horizontal/vertical mixing, deep winter mixing and via aeolian dust estimated as ~ 0.12 µmol m^{-2} d^{-1}. We suggest that additionally required DFe was provided through recycling of biogenically stored Fe following luxury Fe uptake by phytoplankton on the Fe rich shelf. This process would allow Fe to be retained in the surface mixed layer of waters

Biogeosciences Discuss., https://doi.org/10.5194/bg-2017-299
Manuscript under review for journal Biogeosciences
Discussion started: 28 July 2017

downstream of South Georgia through continuous recycling and biological uptake, and facilitate the large scale blooms.

Biogeosciences Discuss., https://doi.org/10.5194/bg-2017-299
Manuscript under review for journal Biogeosciences
Discussion started: 28 July 2017

1. Introduction

The Southern Ocean is the largest 'High Nitrate Low Chlorophyll' (HNLC) region of the global ocean (Buesseler et al., 2004), as a consequence of low iron (Fe) supply and subsequent reduced phytoplankton growth (Buesseler et al., 2004; Tsuda et al., 2009). Iron can be supplied to surface waters of the Southern Ocean by atmospheric dust inputs (Cassar et al., 2007; Gao et al., 2001), horizontal/vertical advection and diffusion from Fe enriched waters (de Jong et al., 2012), resuspension from shelf sediments (Kalnejais et al., 2010; Marsay et al., 2014), melting of icebergs and glaciers (Raiswell et al., 2008), and hydrothermal inputs (German et al., 2016). Despite the overall HNLC status of the Southern Ocean, regions in the wake of islands feature large seasonal phytoplankton blooms; the Fe sources to these blooms are however poorly constrained (de Jong et al., 2012; Planquette et al., 2007; Pollard et al., 2009).

Downstream of the island of South Georgia intense, long-lasting phytoplankton blooms have been observed which extend hundreds of kilometres, and require an enhanced Fe supply. The blooms peak in austral summer (Borrione et al., 2013), stretch over an area of ca. 750,000 km^2 (Atkinson et al., 2001; Korb et al., 2004), and are responsible for the largest dissolved inorganic carbon deficit reported within the Antarctic Circumpolar Current (ACC) (Jones et al., 2015; Jones et al., 2012). As a consequence of the Fe fertilisation the waters in the vicinity of South Georgia support high biomass with abundant krill and higher predators, some of which are exploited commercially (Atkinson et al., 2001; Murphy et al., 2007).

South Georgia forms part of the volcanically active Scotia Arc in the Atlantic sector of the Southern Ocean and is surrounded by a broad 30 to 100 km wide shelf with an average (albeit highly variable) depth of ca. 200 m (Fig. 1). The island is situated between the Antarctic Polar Front (PF) and the Southern ACC Front (SACCF), within the general northeast flow of the ACC (Meredith et al., 2005; Whitehouse et al., 2008). The ACC

Biogeosciences Discuss., https://doi.org/10.5194/bg-2017-299
Manuscript under review for journal Biogeosciences
Discussion started: 28 July 2017

surface waters are enriched in nitrate, phosphate and silicic acid, but strongly depleted in most trace elements, notably Fe and manganese (Mn) (Browning et al., 2014). The large seasonal phytoplankton blooms downstream of South Georgia are thought to be supplied with Fe from the island during the passage of ACC waters (Borrione et al., 2013; Nielsdóttir et al., 2012).

In this study we show the first comprehensive data set of dissolved and (labile) particulate Fe, Mn, and Al in sediments, pore waters, and the water column overlaying the shelf and shelf edge regions of South Georgia. We also include data on the role of krill in new iron supply and recycling in this region (Schmidt et al., 2011; Schmidt et al., 2016). We discuss differences between the various analysed trace metal fractions and quantify dissolved Fe (DFe) fluxes, such as sedimentary pore water efflux, the supply of sediment derived particulate Fe to the surface mixed layer, the efflux of Fe from glacial melting and the supply of Fe by Antarctic krill faecal pellets. Furthermore, we discuss the productivity of the bloom region to the north of South Georgia in the relation of the Fe supply rates.

2. Methods

2.1 Cruises and Sampling

Samples were collected during three research cruises to South Georgia in 2011 (JR247, JC055), and 2013 (JR274). While cruises JR247 and JR274 aimed to examine the pelagic shelf ecosystem by collection of predominantly water samples (and zooplankton during JR247), JC055 explored the composition of sediments on the South Georgia shelf. Cruise JR247 took place in January 2011 on RRS *James Clark Ross*, and 14 sites on the northern shelf and shelf edge of South Georgia were visited (stations 1 – 21; Fig. 1). Suspended particles were collected onto acid cleaned polycarbonate filters (1 µm pore size; Whatman) using in-situ Stand-Alone Pumping Systems (SAPS; Challenger Oceanic) attached

Biogeosciences Discuss., https://doi.org/10.5194/bg-2017-299
Manuscript under review for journal Biogeosciences
Discussion started: 28 July 2017

Biogeosciences Discussions

to a Kevlar wire and deployed at 20 m, 50 m and 150 m depth (Fig. 1, red dots). The filters were rinsed with deionized water (Milli-Q; Millipore), stored at -20°C, and shipped frozen to the National Oceanography Centre Southampton (NOCS).

Subsurface seawater samples were collected by trace metal clean samplers (Ocean Test Equipment (OTE)) at 9 of the 14 SAPS locations (Fig. 1; black stars). Seawater samples were filtered using cartridge filter (0.2 µm Sartobran P300; Sartorius) into acid cleaned 125 mL low-density polyethylene (LDPE) bottles (Nalgene). Unfiltered samples were collected in 125 mL LDPE bottles for analysis of total dissolvable (TD) trace elements. Surface waters from the South Georgia shelf were collected using a tow fish deployed alongside the ship at 3 – 4 m depth. Samples were filtered in-line using a cartridge filer (0.2 µm Sartobran P300; Sartorius) into acid washed 125 mL LDPE bottles. All seawater samples were acidified on-board with ultra clean HNO_3 (15 M UpA grade, Romil) to pH 1.7 (22 µmol H^+ L^{-1}).

In January and February 2013, RRS *James Clark Ross* cruise JR274 revisited South Georgia and collected surface seawater samples covering the shelf, shelf-edge, and open ocean areas around the island. Dissolved and TD surface seawater samples were collected using the tow fish and treated similarly to samples from JR247. For a more detailed description of all sample-handling procedures, please see Supplementary Text S1.

During the RRS *James Cook* cruise JC055 in February 2011, a megacorer (Bowers and Connelly type) was used to collect surface sediment and pore water samples on the South Georgia shelf. Cores representing the intact sediment – water interface were retrieved from three sites on the southern shelf, at water depths of ca. 250 m (S1 – S3) (Fig. 1, blue hexagons). Pore waters were separated by centrifugation under N_2 atmosphere and filtered using cellulose nitrate syringe filters (0.2 µm pore size; Whatman) (Homoky et al., 2012). Conjugate sediments were freeze dried on board and stored at room temperature. A more detailed description of sediment and pore water sample-handling procedures is provided in Supplementary Text S2.

2.2 Trace metal analysis in suspended particles

The labile trace metal fraction of particles was remobilized using a 25% acetic acid solution (glacial SpA, Romil) following Planquette et al. (2011). This fraction is here after referred to as the leachable particulate trace metal fraction (LP). The remaining particles were digested on a hot plate applying a mixture of aqua regia and hydrogen fluoride (Planquette et al., 2011). This fraction will be referred to as the refractory particulate fraction (RP). The particulate trace metal fraction (P) is the sum of leachable particulate (LP) and refractory particulate (RP). All samples were analysed by collision cell inductively coupled plasma - mass spectrometry (ICP-MS) (ThermoFisher Scientific, XSeriesII).

2.3 Trace metal analysis of seawater

The filtered and unfiltered seawater samples were stored for a period of 12 months prior to analysis. Concentrations of dissolved and total dissolvable Fe, Mn, and Al in seawater were determined by off-line pre-concentration and isotope dilution / standard addition ICP-MS (ThermoFisher Scientific Element2 XR) according to Rapp et al. (2017). For a more detailed description of the method and measured reference materials see Supplementary Text S1.

2.4 Trace metal analysis of pore waters and sediments

Sub-samples of the bulk, homogenized sediments were fully dissolved following an aqua regia and combined hydrofluoric/perchloric acid digestion method following Homoky et al. (2011). The acid digests and pore waters were analysed by ICP-optical emission

Biogeosciences Discuss., https://doi.org/10.5194/bg-2017-299
Manuscript under review for journal Biogeosciences
Discussion started: 28 July 2017

spectrometry (OES) (Perkin Elmer Optima 4300DV). For a more detailed description of the method and measured reference materials see Supplementary Text S2.

3. Results & Discussion

3.1 Supply routes of suspended particulate Fe, Mn, and Al

3.1.1 Two particulate trace metal fractions

Two different particulate fractions were obtained from samples collected during JR247; the particulate fraction, P, from suspended particles collected using 1 µm pore size SAPS filters and the leachable particulate fraction from unfiltered seawater samples (LP_{Un}) . LP_{Un} was calculated following Eq. (1):

$$LP_{Un} = \text{total dissolvable (TD)} - \text{dissolved (D; 0.2 µm pore size filters)} \quad (1)$$

Because of the different sampling approaches and filter cut off sizes (1 µm for SAPS and 0.2 µm for dissolved seawater), concentrations of LP_{Un} and P differed at stations. The concentrations of Fe, Mn and Al in the LP_{Un} fraction ($LP_{Un}Fe$, $LP_{Un}Mn$, $LP_{Un}Al$) were slightly lower than the particulate fraction from suspended particles (PFe, PMn, PAl), but showed similar distribution patterns in the water column (Fig. 2, Table 1 and 2). The LP_{Un} corresponded to ca. 63 ± 4 % of the PFe, 83 ± 11% of the PAl and 100 ± 10% of the PMn fractions. The average LP_{Un} trace metal ratios ($LP_{Un}Fe/ LP_{Un}Mn = 33.07 \pm 3.45$ (1 σ) and $LP_{Un}Fe/ LP_{Un}Al = 0.65 \pm 0.10$ (n=69)), were about half of the elemental ratios of suspended particles (PFe/PMn = 68.0 ± 0.6 and PFe/PAl = 1.251 ± 0.042 (n=42) (Fig. 3; Table 1 and 2)).

The lower concentrations of Fe and Al in the LP_{Un} compared to the P fractions suggests that an important fraction of particulate Fe and Al in seawater was not digested during the acidification procedure at pH 1.7 over 12 months. This refractory particulate fraction, which represented ~1/3 of particulate Fe and ~ 1/5 of the particulate Al pool, was likely associated with detrital mineral material that only dissolves during a digestion with aqua regia and hydrogen fluoride. This implies that the fraction of $LP_{Un}Fe$ and $LP_{Un}Al$ was associated to a more labile fraction, such as biogenic and inorganic particles, including oxyhydroxides (Bonneville et al., 2009; Liu and Millero, 1999), and Fe and Al adsorbed onto charged surfaces (Schlosser et al., 2011).

Since P and LP_{Un} displayed similar trends with depth and showed a linear dependencies (Fig. 2 and 3), LP_{Un} was utilized in the following paragraphs as an indicator for the concentration of particulate trace metals at locations were particulate samples could not be retrieved by SAPS, e.g. in surface waters and depths greater than 150 m.

3.1.2 Suspended particles in the water column

Concentrations of PFe, PMn and PAl in the water column ranged between 0.87 – 267 nmol L^{-1}, 0.01 – 3.85 nmol L^{-1}, and 0.60 – 195 nmol L^{-1}, respectively (Fig. 2, Table 2). Concentrations of $LP_{Un}Fe$, $LP_{Un}Mn$ and $LP_{Un}Al$ ranged between 1 – 118 nmol L^{-1}, 0.01 – 100 nmol L^{-1}, and 1 – 141 nmol L^{-1}, respectively (Fig. 2, Table 1). Below the isopycnal density layer 27.05 kg m^{-3} (at ca. 50 – 70 m depth), P and LP_{Un} increased with depth and showed a maximum near the seafloor of e.g. 207 nmol L^{-1} for PFe and 112 nmol L^{-1} for $LP_{Un}Fe$ (#17, Table 2). Most stations on the shelf (bottom depth ≤ 260 m; #9/10, #13, #14, #17, and #21) showed seafloor maxima, in agreement with other shelf studies. For example, Milne et al. (2017) reported concentrations of up to 140 nmol L^{-1} for PFe and 800 nmol L^{-1} for PAl in bottom waters on the west African shelf, and Chase et al. (2005) showed bottom water maxima of up to 400 nmol L^{-1} for $LP_{Un}Fe$ off the Oregon coast.

Strong linear relationships between elements were observed for suspended particles (SAPS) obtained from above and below the isopycnal, with elemental ratios of PFe/PMn = 68.0 ± 0.6 and PFe/PAl = 1.25 ± 0.04 (n=42) (Fig. 3, Table 2). The elemental ratio were comparable to those reported for the earth crust (Fe/Mn = 60.0 ± 0.2 (Wedepohl, 1995)), indicating that suspended particles had a lithogenic source.

The elemental ratios of suspended particles were higher than those for sediments (mean sediment surface layer of S1, S2, S3; SFe/SMn = 51.5 ± 2.4 and SFe/SAl = 0.34 ± 0.02 (Fig. 4, Table 3)). The Fe/Mn ratios among different phytoplankton species show strong variations but are typically much lower (Fe/Mn ~ 1.7 (Ho et al., 2003)) with lower Fe concentrations than terrestrial/sediment particles (cellular concentration of phytoplankton ~ 0.7 mmol kg^{-1} (Ho et al., 2003); upper crust ~ 550 mmol kg^{-1} (Wedepohl, 1995)). A prevalence of biogenic particles in the suspended particle pool would be expected to lower the PFe/PMn ratio in our fully digested samples to values less than 51.5.

It is likely that enhanced scavenging of DFe onto lithogenic/sediment particles increased the Fe to Mn (and Fe to Al) ratio of suspended particles (PFe/PMn = 68.0) compared to sediment particles (SFe/SMn = 51.5). At seawater pH 8, dissolved Fe(III) is rapidly hydrolysed to soluble $Fe(III)(OH)_3$ (< 0.02 µm) which readily accumulates as nanometer sized colloids (0.02 – 0.2 µm) (Liu and Millero, 2002). It has been shown that both soluble and colloidal Fe are attracted by charged surfaces, a process that lowers the overall amount of DFe and simultaneously increases the amount of particulate Fe in seawater over time (Schlosser et al., 2011).

A range of mechanisms delivers suspended particles to the surface waters. These transport mechanisms will be discussed in the following section.

3.1.3 Glacial outflow and zooplankton activity

Whilst most stations on the shelf showed bottom water maxima of suspended particles, at three sampling sites located on the shelf (#18) and shelf edge (#15/16 and #19/20), the particulate trace metal concentrations featured maxima in the top 100 m of the water column (Fig. 2 and 5). At station #19/20, ca. 100 km away from the coast with a water depth of 1741 m, the PFe concentration at 20 m depth was 97 nmol L^{-1}, similar to $LP_{Un}Fe$ (Fig. 5). The elemental ratio PFe/PMn of these samples (e.g. 64.2 for station #19/20, 20 m depth) were close to the average ratio (PFe/PMn = 68.0), indicating that lithogenic particles dominated the suspended particulate pool in these surface waters.

The surface water maxima could have two supply routes: 1) lateral transport of waters containing lithogenic particles from shallow island shelf sediments, and 2) transport of glacial particles following melt processes. The reduced salinities (~32.5) recorded in surface waters in Cumberland Bay and ~50 km offshore of South Georgia (~33.6) (Fig. 6(c)) provide an indication of glacial outflow, melting of icebergs and run-off of melt water streams. Enhanced $LP_{Un}Fe$ concentrations of up to 22 µmol L^{-1} in low salinity surface waters of Cumberland Bay (Fig. 6(a)), are indicative of a meltwater source. The $LP_{Un}Fe$ concentration decreased strongly with increasing distance from the coast, and exhibited an abrupt reduction to 1 – 5 nmol Fe L^{-1} at the shelf edge ca. 100 km offshore. A similar distribution pattern was observed for $LP_{Un}Mn$ (Fig. 6(d)) and $LP_{Un}Al$ (not shown), for cruises JR247 and JR274. Glacial melt has been reported as an important source of particulate material in the vicinity of the Antarctic Peninsula (de Jong et al., 2012). For example, Gerringa et al. (2012) documented elevated total dissolvable Fe concentration of up to 106 nmol L^{-1} near the Pine Island Glacier in the Amundsen Sea, and Raiswell et al. (2008) estimated that per year 1.6 Gmol nanoparticulate Fe, associated to terrigenous particles, are delivered to the Southern Ocean by melting ice.

Locally elevated particulate metal concentrations in surface waters may also be related to production of faecal pellets by swarms of Antarctic krill (*Euphausia superba*) (Schmidt et al., 2016). High abundances of Antarctic krill estimated from acoustic backscattering (Fielding et al., 2014) and large numbers of faecal pellets were observed on the SAPS filters during cruise JR247. The stomach content of Antarctic krill contained up to 80% sediment particles by volume, an observation that was attributed to feeding by these organisms on deep ocean sediments (Schmidt et al., 2011) and glacial flour (Schmidt et al., 2016). Krill thus take up lithogenic particles incidentally during filter feeding on their phytoplankton food and transfer and suspend them in the surface ocean following their ascend through excretion of faecal pellets (Schmidt et al., 2016). The trace metal contents of krill faecal pellets collected during on-board incubation experiments during JR247 ranged between 0.88 – 67.14 µg Fe mg^{-1} dry weight (n = 27) (Table 4). The molar ratios PFe/PMn = 70.5 ± 8.21 and PFe/PAl = 0.48 ± 0.07 were similar to those for LP_{Un} in bottom waters and P in suspended particles (Table 1, 2 and 4), indicating that krill faecal pellets predominately contained sediment and/or glacial flour particles.

3.2 Supply routes of dissolved Fe, Mn, and Al

Concentrations of DFe, DMn, and DAl in the water column showed strong variations and ranged between ca. 0.1 – 7.7 nmol L^{-1}, 0.3 – 2.1 nmol L^{-1} and 0.1 – 18.4 nmol L^{-1}, respectively (Fig. 2, 5 and 7). Dissolved Fe and Mn in the surface waters ranged between 0.1 – 25.9 nmol L^{-1} and 0.1 – 19.6 nmol L^{-1}, respectively, and were highest in Cumberland Bay, and lowest beyond the shelf break (Fig. 6). Dissolved Fe concentrations from this study are in agreement with reported DFe near the Antarctic Peninsula (0.6 – 14.6 nmol L^{-1} (de Jong et al., 2012)) and Crozet Islands (0.1 – 2.5 nmol L^{-1} (Planquette et al., 2007)). Sources and sinks of dissolved trace metals, and their distribution in the water column are discussed in the following sections.

3.2.1 Supply from sediment pore waters

Biogeosciences Discuss., https://doi.org/10.5194/bg-2017-299
Manuscript under review for journal Biogeosciences
Discussion started: 28 July 2017

Elevated pore water concentrations of Fe and Mn (Fe_{PW} and Mn_{PW}) were observed in sediments from shelf sites at water depths of around 250 m, and ranged between 0.5 – 110 µmol kg^{-1} for Fe and 0.1 – 2 µmol kg^{-1} for Mn (Fig. 7 and Table S2). The down-core distributions of Fe_{PW} and Mn_{PW} were consistent with microbial dissimilatory Mn and Fe reduction during organic matter oxidation (Canfield and Thamdrup, 2009), and thus concentrations were elevated at defined depth horizons controlled by their redox potential (Eh) (Bonneville et al., 2009; Raiswell and Canfield, 2012). The Fe_{PW} and Mn_{PW} concentrations near the sediment-seawater interface were used to calculate fluxes of Fe and Mn to bottom waters following diffusion of reduced Fe and Mn species across an oxygenated layer in surface sediments. These calculations were performed following Boudreau and Scott (1978) and Homoky et al. (2012), and are described in detailed in the Supplementary material (Text S3 and Table S1). We are aware that our calculated fluxes represent minimum estimates of pore water efflux, which under natural conditions is supplemented by advection due to bioirrigation, bioturbation, and bottom water currents (Homoky et al., 2016).

We calculated substantial benthic fluxes from sediment pore waters to bottom waters for Fe_{PW} of <0.1 to 44.4 µmol m^{-2} d^{-1} and Mn_{PW} of 0.6 to 4.1 µmol m^{-2} d^{-1}. The upper flux values for Fe are comparable to those reported for dysoxic and river-dominated continental margins (3.5 – 55 µmol m^{-2} d^{-1} (Homoky et al., 2012)), seasonal maxima of temperate and oxic shelf seas (23 – 31 µmol m^{-2} d^{-1} (Klar et al., 2017)), and shelf sediments off the Antarctic Peninsula (1.3 – 15.5 µmol m^{-2} d^{-1} (de Jong et al., 2012)). The Mn fluxes were relatively low for shelf environments, with for example fluxes of 70 – 4450 µmol m^{-2} d^{-1} reported for Baltic and Black Sea sediments (Pakhomova et al., 2007)). The substantial Fe pore water fluxes from the South Georgia shelf sediments, which extend over an area of ca. 40,000 km^2, indicate that these may serve as an important year-round source to overlying waters, totalling 4 to 1,728 kmol DFe d^{-1} and 25 to 164 kmol DMn d^{-1}.

Benthic release of trace metal enriched pore waters shaped the distributions of dissolved trace metals in bottom waters on the shelf. Concentrations of DFe, DMn, and DAl were enhanced at isopycnals > 27.05 kg m^{-3} (e.g. DFe up to 7.70 nmol L^{-1} at station #21, Table 1) compared to surface waters (e.g. DFe as low as 0.30 nmol L^{-1} at #13, Table 1; Fig. 2 and 7). Trace metal enriched bottom waters were also observed at site #13, #14, #17 and #18 (Fig. 2). The molar DFe/DMn ratios in oxygenated bottom waters varied between 1.1 – 3.5 and were thus similar to pore waters (0 – 1 cm depth) near the sediment-seawater interface (Fe_{PW}/Mn_{PW} = 2.2 ± 1.0; Fig. 7). The similar trace metal ratios suggests that Fe and Mn in enriched pore waters crossed the sediment-bottom water interface and accumulated in shelf bottom waters.

To determine the vertical DFe fluxes from near bottom to surface waters we employed a method outlined by de Jong et al. (2012), and calculated both the advective and diffusive flux terms. Applying literature values for vertical diffusivity (K_Z = 1 x 10^{-4} m^2 s^{-1} (Charette et al., 2007)) and upwelling velocity (w = 1.1 x 10^{-6} m s^{-1} (de Jong et al., 2012)) yielded an average vertical DFe flux on the shelf of 0.41 ± 0.26 µmol m^{-2} d^{-1} from subsurface waters into the surface mixed layer (Supplementary Text S4). The surface mixed layer depth was determined by a density criteria (~0.03 kg m-3 (de Boyer Montégut et al., 2004)) and was located ca. 50 m depth. About 38% of the DFe flux was related to Ekman upwelling (advective term) and 62% to the diffusive flux. This vertical flux is at the lower end of the calculated benthic flux from this study (Fe_{PW} < 0.1 to 44.4 µmol m^{-2} d^{-1}), and agrees with values reported for other Southern Ocean shelf regions near the Antarctic Peninsula (within 20 – 70 km from the coast: ~ 2.7 ± 3.4 µmol m^{-2} d^{-1} (de Jong et al., 2012)) and the Crozet Islands (only diffusive flux of 0.06 µmol m^{-2} d^{-1} (Planquette et al., 2007)).

3.2.2 DFe supply from suspended particles

The analytical protocol for analysis of the particulate material obtained using SAPS yielded refractory and leachable fractions (RP and LP, respectively). The RP fraction of the suspended matter is considered to include silicates and aged oxide minerals, and the LP fraction represents predominantly oxyhydroxides, biogenic material and loosely bound surface associated elements which are readily remobilized using leaching procedures (Berger et al., 2008).

Concentrations of LPFe, LPMn and LPAl in the water column showed strong variations, ranging from a few picomoles to several nanomoles L^{-1} (Table 2). On average, LPFe and LPAl concentrations at 150 m depth (~ 1.3 nmol LPFe L^{-1} and ~0.95 nmol LPAl L^{-1}) were significantly higher than at 20 and 50 m (LPFe = 0.3 nmol L^{-1} (student t-test: t(0.95;28) = 1.725 (1.703)); LPAl = 0.43 nmol L^{-1} (student t-test: t(0.90;28) = 1.383 (1.313))). The LPMn concentrations did not change strongly and remained near constant throughout the top 150 m (LPMn = 8.9 pmol L^{-1} (student t-test: (0.65;28) = 0.400 (0.390))). The average contribution of LP to the particulate pool was low; 0.83 ± 1.13% for Fe, 2.55 ± 1.58% for Mn and 2.42 ± 1.32% for Al (Table 2). A study conducted in the North Pacific near the Columbia River outflow reported considerably higher LP fractions (e.g. 6.6±3.0% of Fe, 78.7±14.0% of Mn, 6.3±2.0% of Al (Berger et al., 2008)), which was attributed to enhanced biogenic particle levels in the low salinity waters of the river (Berger et al., 2008). In contrast, results from our study showed that particulate trace metals mainly had a refractory component (RP), indicating that Fe, Mn, and Al was mainly incorporated in lithogenic material.

A weak linear relationship between RP and LP was observed for Fe (R^2 = 0.57), Mn (R^2 = 0.64) and Al (R^2 = 0.63) (Supplementary Fig. S1), indicating that the LP fraction included mainly Fe, Mn and Al that was scavenged onto lithogenic particle surfaces and not much LPFe was incorporated in biogenic particles. The scavenging of dissolved trace metals by charged particle surfaces is established (Homoky et al., 2012; Koschinsky et al., 2003), but how well Fe and other trace metals can be remobilized from marine particle surfaces and which process may modify their availability over time is not yet constrained.

Freshly produced inorganic Fe(III) oxyhydroxide precipitates in seawater are subject to chemical and structural conversions that lead to less soluble particles with time (Yoshida et al., 2006). Scavenged Fe is however also reported to buffer DFe concentrations in the water column of the tropical Atlantic (Milne et al., 2017). Furthermore, recent work has indicated that zooplankton grazing and the production of faecal pellets remobilizes DFe from lithogenic and biogenic particles (Giering et al., 2012; Riley et al., 2012; Schmidt et al., 2016).

3.2.3 DFe supply from Antarctic krill

Elevated dissolved trace metal concentrations in the top 200 m of the water column coincided with elevated particulate concentrations at stations #11/12, #15/16, #18, and #19/20 (Fig. 2, 5, and 7). The SAPS filters from these stations contained a high load of krill faecal pellets. To elucidate the relationship between dissolved trace metal concentrations and abundance of Antarctic krill and krill faecal pellets, krill were caught and incubated on-board the vessel as described in Schmidt et al. (2016).

Krill excretion rates of DFe were variable, relating positively to recent ingestion of diatoms. However, on average krill released ~2.0 ± 1.9 nmol DFe individual^{-1} d^{-1} (Schmidt et al., 2016). By applying an average Antarctic krill abundance of 465 ± 588 individuals m^{-2}, estimated from acoustic backscattering (Fielding et al., 2014), krill excreted 1.1 ± 2.2 µmol DFe m^{-2} d^{-1} into the top 300 m of the water column (Schmidt et al., 2016). In addition, krill produced ca. 1.8 ± 1.6 mg of faecal pellets per individual per day. Particle leaches performed on those faecal pellet samples with 25% acetic acid showed that on average 2.5 ± 2.1% of the total Fe in these pellets could be remobilised (Table 4), which would equate to a production

Biogeosciences Discuss., https://doi.org/10.5194/bg-2017-299
Manuscript under review for journal Biogeosciences
Discussion started: 28 July 2017

of 14 ± 24 nmol LPFe ind^{-1} d^{-1}. By multiplying the mean LPFe by the ambient krill density used above, we calculate a LPFe flux of 6.5 ± 8.2 µmol m^{-2} d^{-1} from the faecal pellets to the water column.

Since krill are mobile animals, questions remain over where the major part of the LPFe flux occurs, and what the fate of this Fe source is. Highest krill abundances were recorded generally (but not exclusively) in the top 100 m layer (Fielding et al., 2014), and hence a large proportion of this LPFe flux from krill is likely to occur in the upper waters. Notwithstanding our current uncertainties over the depths of origin and fate, the LPFe flux from krill fecal pellets and the release of DFe were on average an order of magnitude higher than the vertical diffusive and advective DFe flux from below, illustrating the potential importance of zooplankton-mediated-Fe-cycling, in agreement with previous studies (Hutchins and Bruland, 1994; Sato et al., 2007).

3.3 Off-shore transport of trace metal enriched water masses

Along the NE – SW transect (Fig. 1; #11/12 via # 13 to #14), lateral water mass transport carried suspended particles offshore. Indeed, elevated concentrations of the P and LP_{Un} metal fractions were observed in subsurface waters that had been in recent contact with the shelf. These metal enriched waters, detected at the eastern shelf edge station #11/12 between 200 and 400 m water depth (Fig. 1 and 4), exhibited similar temperature and salinity signatures to shelf bottom waters. Furthermore, the elemental ratios of the LP_{Un} fraction in these waters were similar to the particles in the surface sediments (S1, S2, and S3) and the resuspended particles in the bottom boundary layer (#13 and #14) on the shallow shelf (Fig. 4). A similar distribution was also found for the P fractions, but limited to station #13 and #14, as SAPS were not deployed below 150 m at the shelf edge location #11/12.

The $LP_{Un}Fe$ concentration decreased exponentially with distance from the island to the offshore: ($P_{Un}Fe = 267.7 * e^{-0.047*d}$, R^2 = 0.999), from station #14 in 200 m depth ($P_{Un}Fe$ = 82.26 nmol L^{-1}) to #13 in 100 m depth ($P_{Un}Fe$ = 34.06 nmol L^{-1}) to #11/12 between 200 and 400 m depth ($P_{Un}Fe$ = 10.18 nmol L^{-1}) (Table 1). The variable *d* represents the distance to the coast in kilometres. A similar exponential decrease was observed for the SAPS data: ($PFe = 125.02 * e^{-0.056*d}$, R^2 = 1), from station #14 (PFe = 31.12 nmol L^{-1}) to #13 (PFe = 10.23 nmol L^{-1}). The decrease of P and LP_{Un} with increasing distance to the coast is in agreement with previous observations in the Western Subarctic Pacific (Lam and Bishop, 2008), which reported elevated LPFe concentrations in the range between 0.6 and 3 nmol L^{-1} in subsurface waters between 100 and 200 m depth along the Kamchatka shelf and related this observation to offshore water mass transport.

Consistent with the observed P and LP_{Un} distributions, elevated dissolved metal concentrations at depths between 200 and 400 m at station #11/12 indicated that trace metal enriched shelf bottom waters were transported offshore (Fig. 7). For horizontal flux calculations we used the entire DFe data set for water depth between 100 and 400 m. However, average DFe concentrations in this depth range were highly variable and did not follow an exponential or power law function with distance from the coast (Fig. S3), which is necessary to determine scale length and horizontal diffusivity (K_h) (de Jong et al., 2012). As a result, horizontal flux calculations from the data could not be executed. Even though flux estimate for this study are not available, the overall distribution of DFe in surface waters might help to determine the horizontal transport of DFe across the shelf break.

The distribution of dissolved trace metals in surface waters indicated that a limited transfer of DFe beyond the shelf break into the bloom region. Surface samples showed that DFe concentrations were strongly enriched in surface waters on the shelf (0.3 – 25.9 nmol L^{-1}, Fig. 6(b)), while DFe concentrations beyond the shelf break decreased abruptly to

Biogeosciences Discuss., https://doi.org/10.5194/bg-2017-299
Manuscript under review for journal Biogeosciences
Discussion started: 28 July 2017

concentrations below 0.2 nmol L^{-1} (Fig. 6(b)). This indicates that DFe was quickly removed from ACC surface waters following passage of the island. However, previous studies in the region indicated DFe transfer beyond the shelf break of South Georgia (Borrione et al., 2013; Nielsdóttir et al., 2012). Nielsdóttir et al. (2012) reported surface waters downstream the island shelf with up to 2 nmol L^{-1} DFe, with seasonal variations and highest concentrations during austral summer in January/February 2008. Dissolved Fe data from JR247 (2011) and JR274 (2012) were also obtained during the summer season, but indicated rapid reduction in DFe concentrations through mixing, biological uptake and/or particle scavenging.

3.4 Iron budget in the bloom region

Large seasonal phytoplankton blooms downstream of South Georgia recorded by earth observing satellites are initiated by Fe supplied from the South Georgia island/shelf system during the passage of ACC waters (Fig. 1) (Borrione et al., 2013; Nielsdóttir et al., 2012). Based on our study, the main DFe sources during this passage of the ACC were benthic release and vertical mixing, release of DFe from krill and krill faecal pellets, and supply of particles from run-off and glacial meltwater. In the following sections we will discuss the strength of each DFe source in the bloom region ca. 1,250 km downstream of the island and estimate how much DFe is required to stimulate the elevated primary productivity in that region.

3.4.1 Phytoplankton Fe requirements in the blooming region

The surface ocean in the vicinity of South Georgia during the austral summer features strongly elevated biomass production (Gilpin et al., 2002) and represents the largest known CO_2 sink in the ACC (12.9 mmol C m^{-2} d^{-1} (Jones et al., 2012)). The Fe requirements of the phytoplankton community in the austral summer within the bloom ca. 1,250 km downstream the island were estimated by combining satellite-derived marine primary productivity data (62 ± 21 mmol C m^{-2} d^{-1} (Ma et al., 2014)) with an average intracellular Fe:C ratio obtained from five Southern Ocean diatom species (5.23 ± 2.84 µmol Fe mol^{-1} C (Strzepek et al., 2011)). This approach yielded an approximate Fe requirement of 0.33 ± 0.11 µmol Fe m^{-2} d^{-1} for the phytoplankton community (Fig. 8). For a more detailed description of the applied values and calculations see Supplementary Text S4.

3.4.2 Horizontal and vertical mixing

De Jong et al. (2012) reported that horizontal and vertical advective, diffusive (diapycnal) and deep winter mixing downstream (1,250 – 1,570 km) of the Antarctic Peninsula (between 51°S and 59°S) supplied DFe to the surface waters in quantities that exceeded the DFe requirement of primary producer (0.13 ± 0.04 µmol DFe m^{-2} d^{-1}) during austral summer. In their study region, de Jong et al. (2012) determined that ca. 0.30 ± 0.22 µmol DFe m^{-2} d^{-1} were supplied by horizontal and vertical fluxes, of which 91% of the vertical flux were attributed to Ekman upwelling (advective term), and 43% of the entire DFe flux was supplied by deep winter mixing. Tagliabu et al. (2014) reported similar model estimates for the region that is located south of the Polar Front and characterized by strong Ekman upwelling and winter entrainment.

For the bloom region downstream of South Georgia model calculations by Tagliabue et al. (2014) indicated that less than 0.0003 µmol DFe m^{-2} d^{-1} were supplied by diapycnal mixing, and ca. -0.0028 µmol DFe m^{-2} d^{-1} were removed by Ekman downwelling. For the vertical flux component, this yields an overall loss of DFe of -0.0025 µmol DFe m^{-2} d^{-1} in the blooming region north of South Georgia (Fig. 8).

Because our horizontal flux calculations were invalid, we applied the horizontal flux estimates from de Jong et al. (2012) for our own Fe budget. For a region ca. 1,250 km

Biogeosciences Discuss., https://doi.org/10.5194/bg-2017-299
Manuscript under review for journal Biogeosciences
Discussion started: 28 July 2017

downstream of a source, calculations according to de Jong et al. (2012) indicate that ca. 0.11 ± 0.03 µmol DFe m^{-2} d^{-1} are supplied to the bloom region by horizontal advection and diffusion (Fig. 8).

3.4.3 Deep winter mixing

The entrainment of new DFe during winter represents an important Fe source to surface waters in the Southern Ocean (de Jong et al., 2012; Tagliabue et al., 2014). Elevated DFe concentrations in subsurface waters support primary production in the austral spring following entrainment by deep winter mixing. Model estimates showed that DFe supplied by winter mixing together with diapycnal mixing matches the Fe requirements at most low productivity sites in the Southern Ocean. However, deep winter mixing at the high productive sites north of South Georgia supplies only ca. 0.011 µmol m^{-2} d^{-1} (Tagliabue et al., 2014) (Fig. 8). Later in the season primary productivity in surface waters is considered to rely strongly on Fe derived from recycling of biogenic material (Boyd et al., 2015).

3.4.4 Dust deposition

Dissolved Fe supplied by the deposition of aeolian dust is considered to be an important source to the Southern Ocean (Conway et al., 2015; Gabric et al., 2010; Gassó and Stein, 2007). Aeolian flux estimates, applied by Borrione et al. (2013) for their South Georgia regional model, suggested that up to 8 µmol Fe m^{-2} d^{-1} are delivered to the bloom regions downstream of South Georgia by dry and wet deposition. However, reliable dry and wet deposition estimates for the Southern Ocean are limited. Data from the South Atlantic along 40°S, ca. 600 nm north of South Georgia, showed that rather low levels of DFe (~ 0.002 µmol m^{-2} d^{-1}) are supplied by dry deposition (Chance et al., 2015). On the other hand, ca. 1.0 ± 1.2 µmol DFe m^{-2} d^{-1} are delivered sporadically to the 40°S area by wet deposition (Chance et al., 2015). However, even when assuming that similar wet deposition fluxes

Biogeosciences Discuss., https://doi.org/10.5194/bg-2017-299
Manuscript under review for journal Biogeosciences
Discussion started: 28 July 2017

occur north of South Georgia, fertilization with DFe is temporally and spatially limited. Furthermore, it is very unlikely that such sporadic events could cause long-lasting and far extending phytoplankton blooms strictly constrained between the PF and the SACCF.

3.4.5 Luxury Fe uptake on the shelf

Vertical/horizontal mixing, deep winter entrainment and dust deposition together supply significantly less DFe (< 0.12 µmol Fe m^{-2} d^{-1}) into the bloom region than the phytoplankton community requires (~ 0.33 µmol Fe m^{-2} d^{-1}) (Fig. 8). The missing supply of ca. 0.21 µmol DFe m^{-2} d^{-1} is likely laterally supplied to the bloom region through advecting phytoplankton cells that are enriched in labile Fe. It has been demonstrated that Fe-rich biogenic particles can be created by luxury iron uptake of diatoms (Iwade et al., 2006; Marchetti et al., 2009). Using bottle incubation experiments, Iwade et al. (2006) showed that under high Fe conditions the coastal diatom *Chaetoceros sociale* stores more intracellular Fe than needed for the production of essential enzymes and proteins. We therefore suggest that phytoplankton cells that grew under excess nutrient supply on the South Georgia shelf stored more Fe than needed for their metabolic processes and that via remineralisation this iron is remobilised in surface waters and made available for phytoplankton uptake.

High recycling efficiencies, described by the f*e* ratio (Boyd et al., 2005), are required to maintain the cycle of remineralisation and uptake in the euphotic zone. This counteracts the loss of particulate Fe by vertical export. Boyd et al. (2015) reported the highest recycling efficiencies of ca. 90% for cold and low-DFe waters such as downstream of South Georgia. Further, these workers showed that the degree of recycling is controlled by the abundance of bacteria with a high Fe quota, such as prokaryotic cyanobacteria, and particularly by grazing zooplankton. The waters off South Georgia feature among the highest biomasses worldwide of metazoan grazers; (Atkinson et al., 2001). These large grazers, chiefly copepods and krill,

Biogeosciences Discuss., https://doi.org/10.5194/bg-2017-299
Manuscript under review for journal Biogeosciences
Discussion started: 28 July 2017

are able to ingest large, Fe rich diatoms (Atkinson, 1994; Hamm et al., 2003), thereby disintegrating cell membranes and releasing trace metals.

In recent years it has become apparent that the recycling of biogenic particles in the euphotic zone is a critical mechanism that maintains primary production, especially when the dissolved nutrient pools become exhausted (Boyd et al., 2015; Tagliabue et al., 2014). However, uncertainties remain to the degree to which Fe is lost during each cycle of uptake and remineralisation. Thus more research is needed, especially field work that encompasses the community structures (bacteria, phytoplankton, zooplankton, and higher predators (Ratnarajah et al., 2017; Wing et al., 2014)), the degree of recycling for macro- and micro-nutrients in the euphotic zone, and loss of Fe through vertical export.

4. Conclusions

Shelf sediment-derived Fe and Fe released from Antarctic krill controls the DFe distribution in the shelf waters around South Georgia. Nevertheless, DFe enriched in shelf waters are not effectively advected to the phytoplankton bloom region downstream of the island. Together with other Fe supplies, such as aeolian dust, deep winter mixing and diapycnal mixing, the horizontal advection contributes insufficiently to the Fe requirements of the bloom.

The majority of the Fe appears to be derived from remineralisation of Fe enriched phytoplankton cells/biogenic particles that are transported with the water masses into the bloom region.

In the 1920s the scientists of the Discovery Investigations speculated that micro-nutrients were responsible for the high productivity near South Georgia (Hardy and Gunther, 1935). Identifying the cause of South Georgia productivity is important because the conditions around this island are changing rapidly. Summer water temperatures have increased by more than 0.9°C since the 1920s (Whitehouse et al., 1996). Glaciers are in retreat (Cook et al., 2010; Hodgson et al., 2014) and populations of larger zooplankton (Atkinson et al., 2004) and higher predators (Forcada and Hoffman, 2014; Murphy et al., 2007) have diminished substantially. Each of the potential nutrient sources may change differently, for example glacial outflow will change non-linearly in a changing climate and the increase in positive Southern Annular Mode anomalies in recent decades (Gillett and Fyfe, 2013) indicates increasing westerlies that may transport more Aeolian dust to the Southern Ocean. While we highlight the importance of grazers and the cycling of various particulate Fe phases in the Fe-fertilisation of the South Georgia bloom, more work is needed to clarify the transport mechanisms of dissolved and particulate Fe.

Author contribution

CS, KS, EA and AA designed the experiments for JC247. CS, MP and AAt carried the experiment out during JC247 and CS and MC analysed the trace metal samples at NOCS. EA carried the experiment out during JC274. Samples from JC274 were analysed by CS and MC. AAq, WH and RM designed the experiments for JR55 and AAq analysed the samples. CS prepared the manuscript with contributions from all co-authors.

Acknowledgements

We would like to thank the officers and crew of RRS *James Clark Ross* for assistance with the pelagic sampling and those of RRS *James Cook* for the benthic coring. This work forms part of the NERC-AFI grant AFI9/07 to AA and EA (NE/F01547X/1). RAM was funded by NERC grants NE/01249X/1 and NE/H004394/1. WBH was supported by NERC fellowship NE/K009532/1

Biogeosciences Discuss., https://doi.org/10.5194/bg-2017-299
Manuscript under review for journal Biogeosciences
Discussion started: 28 July 2017

References

Atkinson, A.: Diets and feeding selectivity among the epipelagic copepod community near South Georgia in summer, Polar Biol., 14, 551-560, 1994.

Atkinson, A., Siegel, V., Pakhomov, E., and Rothery, P.: Long-term decline in krill stock and increase in salps within the Southern Ocean, Nature, 432, 100-103, 2004.

Atkinson, A., Whitehouse, M. J., Priddle, J., Cripps, G. C., Ward, P., and Brandon, M. A.: South Georgia, Antarctica: a productive, cold water, pelagic ecosystem, Mar. Ecol.-Prog. Ser., 216, 279-308, 2001.

Berger, C. J. M., Lippiatt, S. M., Lawrence, M. G., and Bruland, K. W.: Application of a chemical leach technique for estimating labile particulate aluminum, iron, and manganese in the Columbia River plume and coastal waters off Oregon and Washington, J. Geophys. Res., 113, 1-16, 2008.

Bonneville, S., Behrends, T., and Van Cappellen, P.: Solubility and dissimilatory reduction kinetics of iron(III) oxyhydroxides: A linear free energy relationship, Geochim. Cosmochim. Act., 73, 5273-5282, 2009.

Borrione, I., Aumont, O., Nielsdottir, M. C., and Schlitzer, R.: Sedimentary and atmospheric sources of iron around South Georgia, Southern Ocean: a modelling perspective, Biogeosciences Discuss., 10, 10811-10858, 2013.

Boudreau, B. P. and Scott, M. R.: A model for the diffusion-controlled growth of deep-sea manganese nodules, Americ. J. Sc., 278, 903-929, 1978.

Boyd, P. W., Law, C. S., Hutchins, D. A., Abraham, E. R., Croot, P. L., Ellwood, M., Frew, R. D., Hadfield, M., Hall, J., Handy, S., Hare, C., Higgins, J., Hill, P., Hunter, K. A., LeBlanc, K., Maldonado, M. T., McKay, R. M., Mioni, C., Oliver, M., Pickmere, S., Pinkerton, M., Safi, K., Sander, S., Sanudo-Wilhelmy, S. A., Smith, M., Strzepek, R., Tovar-Sanchez, A., and Wilhelm, S. W.: FeCycle: Attempting an iron biogeochemical budget from

Biogeosciences Discuss., https://doi.org/10.5194/bg-2017-299
Manuscript under review for journal Biogeosciences
Discussion started: 28 July 2017

a mesoscale SF6 tracer experiment in unperturbed low iron waters, Global Biogeochem. Cycles, 19, 1-13, 2005.

Boyd, P. W., Strzepek, R. F., Ellwood, M. J., Hutchins, D. A., Nodder, S. D., Twining, B. S., and Wilhelm, S. W.: Why are biotic iron pools uniform across high- and low-iron pelagic ecosystems?, Global Biogeochem. Cycles, 29, 1028-1043, 2015.

Browning, T. J., Bouman, H. A., Henderson, G. M., Mather, T. A., Pyle, D. M., Schlosser, C., Woodward, E. M. S., and Moore, C. M.: Strong responses of Southern Ocean phytoplankton communities to volcanic ash, Geophys. Res. Lett., 41, 1-7, 2014.

Buesseler, K. O., Andrews, J. E., Pike, S. M., and Charette, M. A.: The Effects of Iron Fertilization on Carbon Sequestration in the Southern Ocean, Science, 304, 414-417, 2004.

Canfield, D. E. and Thamdrup, B.: Towards a consistent classification scheme for geochemical environments, or, why we wish the term 'suboxic' would go away, Geobiol., 7, 385-392, 2009.

Cassar, N., Bender, M. L., Barnett, B. A., Fan, S., Moxim, W. J., Levy II, H., and Tilbrook, B.: The Southern Ocean Biological Response to Aelian Iron Input, Science, 317, 1067-1070, 2007.

Chance, R., Jickells, T. D., and Baker, A. R.: Atmospheric trace metal concentrations, solubility and deposition fluxes in remote marine air over the south-east Atlantic, Mar. Chem., 177, 45-55, 2015.

Charette, M. A., Gonneea, M. E., Morris, P., Statham, P., Fones, G., Planquette, H., Salter, I., and Garabato, A. N.: Radium isotopes as tracers of iron sources fueling a Southern Ocean phytoplankton bloom, Deep-Sea Res. II, 54, 1989-1998, 2007.

Chase, Z., Hales, B., Cowles, T., Schwartz, R., and van Geen, A.: Distribution and variability of iron input to Oregon coastal waters during the upwelling season, J. Geophys. Res., 110, 1-14, 2005.

Conway, T. M., Wolff, E. W., Rothlisberger, R., Mulvaney, R., and Elderfield, H. E.: Constraints on soluble aerosol iron flux to the Southern Ocean at the Last Glacial Maximum, Nat. Commun., 6, 1-9, 2015.

Cook, A. J., Poncet, S., Cooper, A. P. R., Herbert, D. J., and Christie, D.: Glacier retreat on South Georgia and implications for the spread of rats, Antarct. Sci., 22, 255-263, 2010.

de Boyer Montégut, C., Madec, G., Fischer, A. S., Lazar, A., and Iudicone, D.: Mixed layer depth over the global ocean: An examination of profile data and a profile-based climatology, J. Geophys. Res., 109, 1-20, 2004.

de Jong, J., Schoemann, V., Lannuzel, D., Croot, P., de Baar, H. J. W., and Tison, J. L.: Natural iron fertilization of the Atlantic sector of the Southern Ocean by continental shelf sources of the Antarctic Peninsula, J. Geophys. Res., 117, 1-25, 2012.

Fielding, S., Watkins, J. L., Trathan, P. N., Enderlein, P., Waluda, C. M., Stowasser, G., Tarling, G. A., and Murphy, E. J.: Interannual variability in Antarctic krill (Euphausia superba) density at South Georgia, Southern Ocean: 1997–2013, ICES J. Mar. Sci., 2014. 1-11, 2014.

Forcada, J. and Hoffman, J. I.: Climate change selects for heterozygosity in a declining fur seal population, Nature, 511, 462-465, 2014.

Gabric, A. J., Cropp, R. A., McTainsh, G. H., Johnston, B. M., Butler, H., Tilbrook, B., and Keywood, M.: Australian dust storms in 2002 and 2003 and their impact on Southern Ocean biogeochemistry, Global Biogeochem. Cycles, 24, 1-17, 2010.

Gao, Y., Kaufman, Y. J., Tanré, D., Kolber, D., and Falkowski, P. G.: Seasonal distributions of aeolian iron fluxes to the global ocean, Geophys. Res. Lett., 28, 29-32, 2001.

Gassó, S. and Stein, A. F.: Does dust from Patagonia reach the sub-Antarctic Atlantic Ocean?, Geophys. Res. Lett., 34, 1-5, 2007.

Biogeosciences Discuss., https://doi.org/10.5194/bg-2017-299
Manuscript under review for journal Biogeosciences
Discussion started: 28 July 2017

German, C. R., Casciotti, K. A., Dutay, J.-C., Heimbürger, L. E., Jenkins, W. J., Measures, C. I., Mills, R. A., Obata, H., Schlitzer, R., Tagliabue, A., Turner, D. R., and Whitby, H.: Hydrothermal impacts on trace element and isotope ocean biogeochemistry, Philos Trans A Math Phys Eng Sci, 374, 1-19, 2016.

Gerringa, L. J. A., Alderkamp, A.-C., Laan, P., Thuróczy, C.-E., De Baar, H. J. W., Mills, M. M., van Dijken, G. L., van Haren, H., and Arrigo, K. R.: Iron from melting glaciers fuels the phytoplankton blooms in Amundsen Sea (Southern Ocean): Iron biogeochemistry, Deep-Sea Res. II, 71-76, 16-31, 2012.

Giering, S. L. C., Steigenberger, S., Achterberg, E. P., Sanders, R., and Mayor, D. J.: Elevated iron to nitrogen recycling by mesozooplankton in the Northeast Atlantic Ocean, Geophys. Res. Lett., 39, L12608, 2012.

Gillett, N. P. and Fyfe, J. C.: Annular mode changes in the CMIP5 simulations, Geophys. Res. Lett., 40, 1189-1193, 2013.

Gilpin, L. C., Priddle, J., Whitehouse, M. J., Savidge, G., and Atkinson, A.: Primary production and carbon uptake dynamics in the vicinity of South Georgia—balancing carbon fixation and removal, Mar. Ecol. Prog. Ser., 242, 51-62, 2002.

Hamm, C. E., Merkel, R., Springer, O., Jurkojc, P., Maier, C., Prechtel, K., and Smetacek, V.: Architecture and material properties of diatom shells provide effective mechanical protection, Nature, 421, 841-843, 2003.

Hardy, A. C. and Gunther, E. R.: The plankton of the South Georgia whaling grounds and adjacent waters, 1926-27, Discovery Reports, 11, 1-456, 1935.

Ho, T.-Y., Quigg, A., Finkel, Z. V., Milligan, A. J., Wyman, K., Falkowski, P. G., and Morel, F. M. M.: The elemental composition of some marine phytoplankton, J. Phycol., 39, 1145-1159, 2003.

Biogeosciences Discuss., https://doi.org/10.5194/bg-2017-299
Manuscript under review for journal Biogeosciences
Discussion started: 28 July 2017

Hodgson, D. A., Graham, A. G. C., Griffiths, H. J., Roberts, S. J., Cofaigh, C. Ó., Bentley, M. J., and Evans, D. J. A.: Glacial history of sub-Antarctic South Georgia based on the submarine geomorphology of its fjords, Quat Sci Rev, 89, 129-147, 2014.

Homoky, W. B., Hembury, D. J., Hepburn, L. E., Mills, R. A., Statham, P. J., Fones, G. R., and Palmer, M. R.: Iron and manganese diagenesis in deep sea volcanogenic sediments and the origins of pore water colloids, Geochim. Cosmochim. Act., 75, 5032-5048, 2011.

Homoky, W. B., Severmann, S., McManus, J., Berelson, W. M., Riedel, T. E., Statham, P. J., and Mills, R. A.: Dissolved oxygen and suspended particles regulate the benthic flux of iron from continental margins, Mar. Chem., 134–135, 59-70, 2012.

Homoky, W. B., Weber, T., Berelson, W. M., Conway, T. M., Henderson, G. M., van Hulten, M., Jeandel, C., Severmann, S., and Tagliabue, A.: Quantifying trace element and isotope fluxes at the ocean–sediment boundary: a review, Philos Trans A Math Phys Eng Sci, 374, 2016.

Hutchins, D. A. and Bruland, K. W.: Grazer-mediated regeneration and assimilation of Fe, Zn and Mn from planktonic prey, Mar. Ecol.-Prog. Ser., 110, 259-269, 1994.

Iwade, S., Kuma, K., Isoda, Y., Yoshida, M., Kudo, I., Nishioka, J., and Suzuki, K.: Effect of high iron concentrations on iron uptake and growth of a coastal diatom Chaetoceros sociale, Aquat. Microb. Ecol., 43, 177-191, 2006.

Jones, E. M., Bakker, D. C. E., Venables, H. J., and Hardman-Mountford, N. J.: Seasonal cycle of CO2 from the sea ice edge to island blooms in the Scotia Sea, Southern Ocean, Mar. Chem., 177, 490-500, 2015.

Jones, E. M., Bakker, D. C. E., Venables, H. J., and Watson, A. J.: Dynamic seasonal cycling of inorganic carbon downstream of South Georgia, Southern Ocean, Deep-Sea Res. II, 59–60, 25-35, 2012.

Biogeosciences Discuss., https://doi.org/10.5194/bg-2017-299
Manuscript under review for journal Biogeosciences
Discussion started: 28 July 2017

Kalnejais, L. H., Martin, W. R., and Bothner, M. H.: The release of dissolved nutrients and metals from coastal sediments due to resuspension, Mar. Chem., 121, 224-235, 2010.

Klar, J. K., Homoky, W. B., Statham, P. J., Birchill, A. J., Harris, E. L., Woodward, E. M. S., Silburn, B., Cooper, M. J., James, R. H., Connelly, D. P., Chever, F., Lichtschlag, A., and Graves, C.: Stability of dissolved and soluble Fe(II) in shelf sediment pore waters and release to an oxic water column, Biogeochemistry, 2017. 1-19, 2017.

Korb, R. E., Whitehouse, M. J., and Ward, P.: SeaWiFS in the southern ocean: spatial and temporal variability in phytoplankton biomass around South Georgia, Deep-Sea Res. II, 51, 99-116, 2004.

Koschinsky, A., Winkler, A., and Fritsche, U.: Importance of different types of marine particles for the scavenging of heavy metals in the deep-sea bottom water, Appl Geochem, 18, 693-710, 2003.

Lam, P. J. and Bishop, J. K. B.: The continental margin is a key source of iron to the HNLC North Pacific Ocean, Geophys. Res. Lett., 35, 1-5, 2008.

Liu, H. and Millero, F. J.: The solubility of iron hydroxide in sodium chloride solutions, Geochim. Cosmochim. Act., 63, 3487-3497, 1999.

Liu, X. and Millero, F. J.: The solubility of iron in seawater, Mar. Chem., 77, 43-54, 2002.

Ma, S., Tao, Z., Yang, X., Yu, Y., Zhou, X., M, W., and Li, Z.: Estimation of marine primary productivity from satellite-derived phytoplankton absorption data, IEEE J-STARS, 7, 3084-3092, 2014.

Marchetti, A., Parker, M. S., Moccia, L. P., Lin, E. O., Arrieta, A. L., Ribalet, F., Murphy, M. E. P., Maldonado, M. T., and Armbrust, E. V.: Ferritin is used for iron storage in bloom-forming marine pennate diatoms, Nature, 457, 467-470, 2009.

Marsay, C. M., Sedwick, P. N., Dinniman, M. S., Barrett, P. M., Mack, S. L., and McGillicuddy, D. J.: Estimating the benthic efflux of dissolved iron on the Ross Sea continental shelf, Geophys. Res. Lett., 41, 7576-7583, 2014.

Meredith, M. P., Brandon, M. A., Murphy, E. J., Trathan, P. N., Thorpe, S. E., Bone, D. G., Chernyshkov, P. P., and Sushin, V. A.: Variability in hydrographic conditions to the east and northwest of South Georgia, 1996–2001, J. Marine Syst., 53, 143-167, 2005.

Milne, A., Schlosser, C., Wake, B. D., Achterberg, E. P., Chance, R., Baker, A. R., Forryan, A., and Lohan, M. C.: Particulate phases are key in controlling dissolved iron concentrations in the (sub)tropical North Atlantic, Geophys. Res. Lett., 44, 2377-2387, 2017.

Murphy, E. J., Trathan, P. N., Watkins, J. L., Reid, K., Meredith, M. P., Forcada, J., Thorpe, S. E., Johnston, N. M., and Rothery, P.: Climatically driven fluctuations in Southern Ocean ecosystems, P ROY SOC B-BIOL SCI, 274, 3057-3067, 2007.

Nielsdóttir, M. C., Bibby, T. S., Moore, C. M., Hinz, D. J., Sanders, R., Whitehouse, M., Korb, R., and Achterberg, E. P.: Seasonal and spatial dynamics of iron availability in the Scotia Sea, Mar. Chem., 130–131, 62-72, 2012.

Pakhomova, S. V., Hall, P. O. J., Kononets, M. Y., Rozanov, A. G., Tengberg, A., and Vershinin, A. V.: Fluxes of iron and manganese across the sediment–water interface under various redox conditions, Mar. Chem., 107, 319-331, 2007.

Planquette, H., Sanders, R., Statham, P. J., Morris, P. J., and Fones, G. R.: Fluxes of particulate iron from the upper ocean around the Crozet Islands: A naturally iron-fertilized environment in the Southern Ocean, Global Biogeochem. Cycles, 25, 1-12, 2011.

Planquette, H., Statham, P. J., Fones, G. R., Charette, M. A., Moore, C. M., Salter, I., Nedelec, F. H., Taylor, S. L., French, M., Baker, A. R., Mahowald, N., and Jickells, T. D.: Dissolved iron in the vicinity of the Crozet Islands, Southern Ocean, Deep-Sea Res. II, 54, 1999-2019, 2007.

Biogeosciences Discuss., https://doi.org/10.5194/bg-2017-299
Manuscript under review for journal Biogeosciences
Discussion started: 28 July 2017

Pollard, R. T., Salter, I., Sanders, R. J., Lucas, M. I., Moore, C. M., Mills, R. A., Statham, P. J., Allen, J. T., Baker, A. R., Bakker, D. C. E., Charette, M. A., Fielding, S., Fones, G. R., French, M., Hickman, A. E., Holland, R. J., Hughes, J. A., Jickells, T. D., Lampitt, R. S., Morris, P. J., Nedelec, F. H., Nielsdottir, M., Planquette, H., Popova, E. E., Poulton, A. J., Read, J. F., Seeyave, S., Smith, T., Stinchcombe, M., Taylor, S., Thomalla, S., Venables, H. J., Williamson, R., and Zubkov, M. V.: Southern Ocean deep-water carbon export enhanced by natural iron fertilization, Nature, 457, 577-580, 2009.

Raiswell, R., Benning, L. G., Tranter, M., and Tulaczyk, S.: Bioavailable iron in the Southern Ocean: the significance of the iceberg conveyor belt, Geochemical Transactions, 9, 1-9, 2008.

Raiswell, R. and Canfield, D. E.: The Iron Biogeochemical Cycle Past and Present, Geochemical Perspectives, 1, 1-2, 2012.

Rapp, I., Schlosser, C., Rusiecka, D., Gledhill, M., and Achterberg, E. P.: Automated preconcentration of Fe, Zn, Cu, Ni, Cd, Pb, Co, and Mn in seawater with analysis using high-resolution sector field inductively-coupled plasma mass spectrometry, Anal. Chimi. Acta, 976, 1-13, 2017.

Ratnarajah, L., Lannuzel, D., Townsend, A. T., Meiners, K. M., Nicol, S., Friedlaender, A. S., and Bowie, A. R.: Physical speciation and solubility of iron from baleen whale faecal material, Mar. Chem., 2017. 2017.

Riley, J. S., Sanders, R., Marsay, C., Le Moigne, F. A. C., Achterberg, E. P., and Poulton, A. J.: The relative contribution of fast and slow sinking particles to ocean carbon export, Global Biogeochem. Cycles, 26, 1-10, 2012.

Sato, M., Takeda, S., and Furuya, K.: Iron regeneration and organic iron(III)-binding ligand production during in situ zooplankton grazing experiment, Mar. Chem., 106, 471-488, 2007.

Schlosser, C., De La Rocha, C. L., and Croot, P. L.: Effects of iron surface adsorption and sample handling on iron solubility measurements, Mar. Chem., 127, 48-55, 2011.

Biogeosciences Discuss., https://doi.org/10.5194/bg-2017-299
Manuscript under review for journal Biogeosciences
Discussion started: 28 July 2017

Schmidt, K., Atkinson, A., Steigenberger, S., Fielding, S., Lindsay, M. C. M., Pond, D. W., Tarling, G. A., Klevjer, T. A., Allen, C. S., Nicol, S., and Achterberg, E. P.: Seabed foreaging by Antarctic krill: Implications for stock assessment, bentho-pelagic coupling, and the vertical transfer of iron, Limnol. Oceanogr., 56, 1411-1428, 2011.

Schmidt, K., Schlosser, C., Atkinson, A., Fielding, S., Venables, H. J., Waluda, C. M., and Achterberg, E. P.: Zooplankton gut passage mobilises lithogenic iron for ocean productivity, Curr. Biol., 26, 1-7, 2016.

Strzepek, R., Maldonado, M. T., Hunter, K. A., Frew, R. D., and Boyd, P. W.: Adaptive strategies by Southern Ocean phytoplankton to lessen iron limitation: Uptake of organically complexed iron and reduced cellular iron requirements, Limnol. Oceanogr., 56, 1983-2002, 2011.

Tagliabue, A., Sallee, J.-B., Bowie, A. R., Levy, M., Swart, S., and Boyd, P. W.: Surface-water iron supplies in the Southern Ocean sustained by deep winter mixing, Nat Geosci, 7, 314-320, 2014.

Tsuda, A., Saito, H., Machida, R. J., and Shimode, S.: Meso- and microzooplankton responses to an in situ iron fertilization experiment (SEEDS II) in the northwest subarctic Pacific, Deep-Sea Res. II, 56, 2767-2778, 2009.

Wedepohl, K. H.: The composition of the continental crust, Geochim. Cosmochim. Act., 59, 1217-1232, 1995.

Whitehouse, M. J., Korb, R. E., Atkinson, A., Thorpe, S. E., and Gordon, M.: Formation, transport and decay of an intense phytoplankton bloom within the High-Nutrient Low-Chlorophyll belt of the Southern Ocean, J. Marine Syst., 70, 150-167, 2008.

Whitehouse, M. J., Priddle, J., and Symon, C.: Seasonal and annual change in seawater temperature, salinity, nutrient and chlorophyll a distributions around South Georgia, South Atlantic, Deep-Sea Res. I, 43, 425-443, 1996.

Wing, S. R., Jack, L., Shatova, O., Leichter, J. J., Barr, D., Frew R. D., and Gault-Ringold, M.: Seabirds and marine mammals redistribute bioavailable iron in the Southern Ocean, Mar. Ecol. Prog. Ser., 510, 1-13, 2014.

Yoshida, M., Kuma, K., Iwade, S., Isoda, Y., Takata, H., and Yamada, M.: Effect of aging time on the availability of freshly precipitated ferric hydroxide to costal marine diatoms, Mar. Biol., 149, 379-392, 2006.

Biogeosciences Discuss., https://doi.org/10.5194/bg-2017-299
Manuscript under review for journal Biogeosciences
Discussion started: 28 July 2017

Biogeosciences Discussions
Open Access
EGU

Table 1: Fe, Mn, and Al concentrations determined for the dissolved (D) (0.2 µm) and the leachable particulate fraction (LP_{UN}) (total dissolvable – dissolved) of unfiltered seawater samples collected during JR247. Additional information covers sampling date, station ID, event number and latitude and longitude.

Date	Station ID	Depth		Leach. Part. (nmol L^{-1})			Dissolved (nmol L^{-1})	
	Lat. & Lon.	(m)	$LP_{Un}Fe$	$LP_{Un}Mn$	$LP_{Un}Al$	DFe	DMn	DAl
04/01/2011	#9/10 (E95 & E97)	20	20.36	0.95	46.41	5.71	1.83	1.11
		50	15.18	0.42	40.86	3.19	1.88	2.27
	54.26°S, 35.35°W	100	9.86	0.23	20.43	1.55	0.92	2.07
		130	23.33	0.73	48.91	2.82	0.87	2.68
		150	23.71	0.43	46.95	2.35	1.03	0.12
		200	27.37	0.62	54.41	2.70	0.89	2.37
05/01/2011	#11/12 (E98 & E101)	20	4.05	0.38	6.68	2.19	0.41	3.57
		35	1.52	0.39	7.28	0.41	0.37	-
	54.62°S, 34.81°W	50	9.30	0.60	22.20	7.18	0.64	13.31
		75	1.28	0.31	7.85	0.77	0.35	4.56
		100	2.02	0.32	3.34	1.09	0.35	1.47
		150	1.55	0.38	3.18	1.10	0.45	-
		200	13.10	1.31	23.81	1.26	1.17	3.07
		300	8.62	0.70	23.25	1.06	0.55	-
		400	8.81	0.54	16.54	2.05	0.46	2.69
		500	4.51	0.41	11.41	0.72	0.38	0.76
		600	2.75	0.37	10.32	0.96	0.36	0.77
		700	4.81	0.41	16.85	0.82	0.35	-
06/01/2011	#13 (E105)	20	3.46	0.62	14.68	0.28	0.57	4.53
		35	1.00	0.33	7.17	0.10	0.28	2.64
	54.53°S, 35.27°W	50	7.09	0.71	22.62	1.26	0.57	5.77
		75	25.03	1.09	61.94	1.23	0.64	5.86
		100	34.06	1.30	87.43	0.82	0.74	4.08
07/01/2011	#14 (E113)	20	4.00	0.89	7.87	0.64	0.85	2.57
		50	2.23	0.31	7.64	0.27	0.32	1.80
	54.56°S, 35.59°W	75	2.30	0.43	3.58	0.62	0.46	2.42
		100	2.26	0.44	3.34	0.35	0.46	0.46
		150	23.50	0.94	33.35	0.70	0.62	0.23
		200	82.26	2.12	103.11	2.69	0.77	2.31
08/01/2011	#15/16 (E119 & E129)	20	17.66	0.46	26.66	0.99	1.36	-
		35	16.60	0.30	13.37	0.96	1.27	-
	53.62°S, 36.34°W	50	16.30	0.23	18.49	1.21	1.40	-
		75	23.82	0.56	29.86	0.98	1.28	-
		100	8.49	0.10	10.50	0.73	0.56	-
		150	1.88	0.03	4.49	2.25	0.40	-
		200	2.72	0.02	1.40	0.63	0.44	2.87

Biogeosciences Discuss., https://doi.org/10.5194/bg-2017-299
Manuscript under review for journal Biogeosciences
Discussion started: 28 July 2017

		300	2.56	0.05	2.40	0.34	0.25	-
		400	3.75	0.02	5.28	0.48	0.30	1.17
		500	5.28	0.08	9.22	0.43	0.30	-
		600	5.50	0.09	11.45	0.53	0.28	1.63
		750	5.27	0.06	8.16	0.44	0.30	-
10/01/2011	#17 (E133)	20	10.92	0.22	7.43	2.31	1.20	3.76
		35	20.83	0.53	16.22	1.81	1.34	2.56
	53.90°S, 36.57°W	50	34.59	1.00	57.55	2.29	1.42	2.33
		75	118.25	2.18	64.36	4.21	1.86	2.19
		100	50.71	1.00	77.52	2.48	1.42	1.62
		150	112.28	2.23	86.09	3.39	1.41	0.86
11/01/2011	#18 (E138)	20	106.71	1.77	95.17	2.75	1.57	3.36
		35	83.53	0.00	100.32	1.97	1.33	2.44
	54.10°S, 36.25°W	50	9.67	0.00	18.23	0.74	0.85	-
		75	5.65	0.00	8.90	0.62	0.65	-
		100	4.50	0.08	23.65	1.25	0.48	5.18
		150	7.81	0.11	12.87	1.43	0.49	8.19
12/01/2011	#19/20 (E141 & E143)	20	60.19	2.11	54.29	1.46	1.71	5.30
		35	60.17	2.19	87.17	1.34	1.90	8.22
	53.54°S, 38.11°W	50	66.78	2.74	141.75	1.57	1.90	8.73
		75	71.69	1.78	79.19	1.61	2.13	11.45
		100	10.77	0.25	32.12	0.99	0.67	10.74
		150	5.43	0.13	31.35	1.84	0.92	12.00
		200	7.92	0.14	27.42	1.45	0.60	9.60
		400	5.35	0.00	23.61	1.61	0.45	18.44
		600	5.81	0.10	35.99	1.06	0.38	10.74
		800	4.26	0.13	35.67	1.07	0.36	11.95
13/01/2011	#21 (E151)	20	44.75	1.54	114.13	0.72	1.38	2.58
		35	39.99	1.82	73.37	0.77	0.94	2.29
	53.75°S, 38.98°W	50	48.57	2.03	94.66	1.24	1.36	1.91
		75	25.63	0.91	68.56	0.98	1.17	-
		100	64.06	1.91	114.03	2.33	1.32	1.51
		150	73.04	1.59	62.83	7.70	1.28	12.20

Biogeosciences Discuss., https://doi.org/10.5194/bg-2017-299
Manuscript under review for journal Biogeosciences
Discussion started: 28 July 2017

Table 2: Particulate Fe (PFe), Mn (PMn), and Al (PAl) concentrations in the top 150 m of the water column at the 14 sites visited during JR247. The leachable particulate fraction (LP) is indicated in percent. Additional information covers sampling date, station ID, event number, latitude and longitude, and water column depth. (Depths marked by * indicate that the polycarbonate filter was corrupted after retrieving the SAPS)

Date	Station ID	Depth		Particulate (nmol L^{-1})			Leach. Part. (%)	
	Lat. & Lon.	(m)	PFe	PMn	PAl	LPFe	LPMn	LPAl
25/12/2010	#1/2 (E22)	20	5.17	0.08	4.82	0.37	2.39	1.65
	53.70°S, 38.21°W	50*	9.12	0.14	7.91	0.27	2.61	1.47
	(322 m)	150*	76.61	1.09	66.91	6.26	2.74	4.65
26/12/2010	#3 (E31)	20	6.62	0.09	6.64	0.02	3.30	0.79
	53.85°S, 39.14°W	50	267.48	3.85	162.59	1.48	0.79	0.65
	(287 m)	150	4.36	0.06	4.26	0.07	1.55	1.93
31/12/2010	#4/5 (E72)	20	8.52	0.12	7.99	0.51	1.68	2.62
	53.49°S, 37.71°W	50	15.15	0.23	12.96	0.56	2.44	2.74
	(1917 m)	150	2.33	0.03	2.15	0.65	1.78	2.42
02/01/2011	#6 (E80)	20	85.74	1.11	59.05	1.60	2.28	4.50
	53.99°S, 36.37°W	50	17.76	0.24	8.87	-	-	-
	(208 m)	150	137.39	2.02	98.54	3.46	0.91	2.81
03/01/2011	#7/8 (E88)	20	1.95	0.02	0.87	0.13	2.97	4.99
	54.10°S, 35.46°W	50	1.67	0.02	0.92	0.08	4.35	4.24
	(330 m)	150	1.23	0.02	0.71	0.19	2.11	5.13
04/01/2011	#9/10 (E96)	20	20.91	0.08	15.74	0.56	5.01	3.24
	54.26°S, 35.35°W	50	19.16	0.27	15.58	0.45	1.22	2.51
	(263 m)	150	54.06	0.77	48.10	1.08	1.65	2.08
05/01/2011	#11/12 (E100)	20*	1.49	0.01	0.86	0.18	4.42	2.92
	54.62°S, 34.81°W	50	0.87	0.01	0.60	0.27	6.63	4.20
	(747 m)	150	1.76	0.03	1.08	0.37	4.38	3.33
06/01/2011	#13 (E106)	20	2.75	0.03	1.78	0.63	3.13	4.29
	54.53°S, 35.27°W	50	4.11	0.05	3.07	0.44	2.04	2.76
	(133 m)	100	10.28	0.15	7.62	0.46	1.70	2.54
07/01/2011	#14 (E114)	20	2.80	0.04	1.84	0.07	1.58	3.29
	54.56°S, 35.59°W	50	1.41	0.02	0.97	0.10	2.57	3.92
	(263 m)	150	31.34	0.46	26.92	0.72	1.57	2.28
08/01/2011	#15/16 (E120)	20	24.54	0.37	22.91	0.85	3.95	1.88
	53.62°S, 36.34°W	50	27.72	0.40	23.23	0.43	3.65	1.36
	(852 m)	150	4.74	0.07	3.94	0.90	4.31	1.06
10/01/2011	#17 (E134)	20	10.43	0.14	8.09	0.34	1.66	2.41
	53.90°S, 36.57°W	50	43.04	0.60	38.79	1.34	1.07	1.67
	(209 m)	150	207.48	3.10	194.88	1.72	0.82	1.50
11/01/2011	#18 (E139)	20	95.52	1.32	88.39	1.39	1.82	1.93

	54.10°S, 36.25°W	50	37.43	0.52	35.33	1.16	1.29	1.85
	(276 m)	150	28.00	0.41	23.60	1.26	2.35	2.27
12/01/2011	#19/20 (E142)	20	97.60	1.52	97.10	0.16	1.66	0.33
	53.54°S, 38.11°W	50	90.96	1.42	92.89	0.39	1.98	0.80
	(1741 m)	150	7.41	0.12	6.37	0.74	8.25	2.75
13/01/2011	#21 (E152)	20	50.75	0.85	52.78	0.06	2.99	0.12
	53.75°S, 38.98°W	50	59.59	0.93	59.98	0.05	2.15	0.09
	(269 m)	150	153.48	2.34	89.63	3.14	1.10	2.94

Biogeosciences Discuss., https://doi.org/10.5194/bg-2017-299
Manuscript under review for journal Biogeosciences
Discussion started: 28 July 2017

Table 3: Particulate iron (SFe), aluminum (SAl), and manganese (SMn) concentrations in shelf sediments collected during JC055 in January and February 2011. Pore water data retrieved additionally from these three cores are listed for Fe (Fe_{PW}) and Mn (Mn_{PW}). Additional information are event number (MC…), latitude and longitude, and water column depth.

Station ID Lat. & Lon.	Depth (cm)	SFe (mol kg-1)	SAl (mol kg-1)	SMn (mmol kg-1)	Fe_{PW} (µmol kg-1)	Mn_{PW} (µmol kg-1)
#S1 (MC33)	0.5	0.58	1.77	11.56	3.01	2.29
54.16°S, 37.98°W	1.5	0.61	1.74	11.52	17.47	0.84
(257 m)	2.5	0.59	1.77	11.78	110.90	0.28
	3.5	0.6	1.86	12.05	106.24	0.53
	4.5	0.58	1.72	11.82	94.09	0.34
	5.5	0.59	1.86	12.04	82.79	0.27
	9	0.56	1.72	11.19	32.98	0.00
	15	0.55	1.74	11.15	2.44	0.06
	25	0.53	1.6	10.81	0.80	0.16
#S2 (MC34)	0.5	0.64	1.77	11.42	1.53	0.87
54.16°S, 37.94°W	1.5	0.6	1.79	11.73	/	/
(247 m)	2.5	0.58	1.76	11.81	0.97	0.24
	6.5	0.59	1.83	12.23	11.19	0.26
	10.5	0.58	1.8	11.78	14.28	0.25
	14.5	0.54	1.6	10.83	3.59	0.33
	16.5	0.56	1.72	11.22	2.27	0.31
#S3 (MC35)	0.5	0.61	1.67	11.42	1.46	0.43
54.15°S, 37.97°W	1.5	0.59	1.76	11.7	28.94	0.35
(254 m)	2.5	0.58	1.76	11.7	91.52	0.37
	3.5	0.59	1.81	12.03	40.16	0.44
	5.5	0.57	1.78	11.58	49.37	0.56
	8.5	0.59	1.82	11.65	67.92	0.52
	17	0.54	1.69	10.8	3.87	0.34
	19	0.55	1.67	10.86	1.82	0.12
	25	0.55	1.77	11.19	2.73	0.36
	29	0.56	1.79	11.19	5.64	0.16

Table 4: Total and leachable particulate Fe, Mn, and Al determined for the 27 individual krill faecal pellet samples collected during 9 krill incubation experiments on-board RRS *James Clark Ross* (JR247).

# Sample	pellet weight (mg)	Total Fe (µg mg^{-1})	Total Al (µg mg^{-1})	Total Mn (ng mg^{-1})	Leach. P. Fe (%)	Leach. P. Al (%)	Leach. P. Mn (%)
1	4.87	0.88	1.06	12.5	6.33	8.83	13.24
2	2.18	1.33	1.68	16.7	3.02	8.81	8.22
3	4.26	1.07	1.90	17.8	5.37	3.27	11.81
4	1.91	5.19	5.53	76.1	2.15	1.95	5.68
5	1.41	2.70	2.84	39.1	2.46	1.59	3.54
7	7.80	67.1	64.2	998.3	2.93	2.21	3.25
8	0.99	2.71	2.42	35.0	3.76	4.59	5.99
10	1.48	6.42	4.89	71.6	0.29	4.83	0.91
13	2.79	4.13	3.11	50.3	0.36	5.07	1.53
15	0.77	37.3	38.1	531.1	2.03	2.80	6.21
16	1.21	6.35	6.22	81.2	1.24	7.47	3.13
18	12.27	40.0	36.6	582.5	3.95	2.07	4.29
19	2.19	11.2	9.49	146.9	0.15	2.03	1.07
22	2.43	48.1	49.7	721.5	0.81	2.32	0.98
40	3.35	22.8	22.0	337.4	5.51	3.21	5.50
41	8.55	6.91	7.14	103.1	1.11	1.88	4.31
42	3.5	25.7	24.8	376.2	5.09	2.98	5.29
45	0.40	3.96	4.43	43.3	1.27	13.90	1.46
47	7.65	3.63	3.92	52.7	0.34	0.68	3.65
48	0.63	3.06	3.21	34.1	0.05	4.22	0.76
49	4.42	29.6	28.5	438.4	1.65	2.93	1.95
50	7.46	2.31	2.37	34.6	0.36	0.51	2.78
51	5.18	28.0	27.1	431.3	1.85	2.60	2.01
62	1.20	4.63	4.68	68.0	0.31	1.78	0.47
68	2.25	44.0	40.2	667.4	4.84	1.95	4.77
69	1.66	43.6	44.8	663.7	5.66	2.13	5.46
71	3.47	35.3	36.4	557.7	1.50	1.99	1.76

Biogeosciences Discuss., https://doi.org/10.5194/bg-2017-299
Manuscript under review for journal Biogeosciences
Discussion started: 28 July 2017

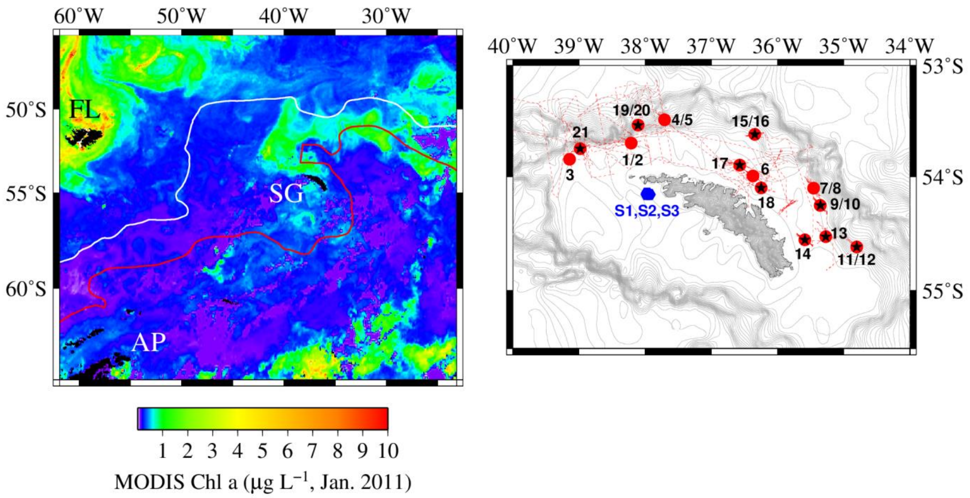

Figure 1: (Left figure) Locations of Falkland Islands (FL), South Georgia (SG), and Antarctic Peninsula (AP) in the Atlantic sector of the Southern Ocean. South Georgia is located between the Antarctic Polar Front (PF, white line) and the Subantarctic Circumpolar Current Front (SACCF, red line). The colour bar represents the Chlorophyll a (Chl a) content recorded by the MODIS satellite in January 2011. (Right figure) The region around SG and the OTE (black stars) and SAPS sampling sites (red points) visited during JR247. The red dashed line illustrates the cruise track of JR247. The three sediment sampling sites S1, S2, and S3 visited during JC055 are shown by blue hexagons. The ocean bathymetry of the region was plotted using the GEBCO bathymetric data set. The shelf of South Georgia is between 100 and 250 m deep and extends about 30 to 100 km (shelf edge indicated by high density of isobaths).

Biogeosciences Discuss., https://doi.org/10.5194/bg-2017-299
Manuscript under review for journal Biogeosciences
Discussion started: 28 July 2017

Biogeosciences
Discussions
Open Access

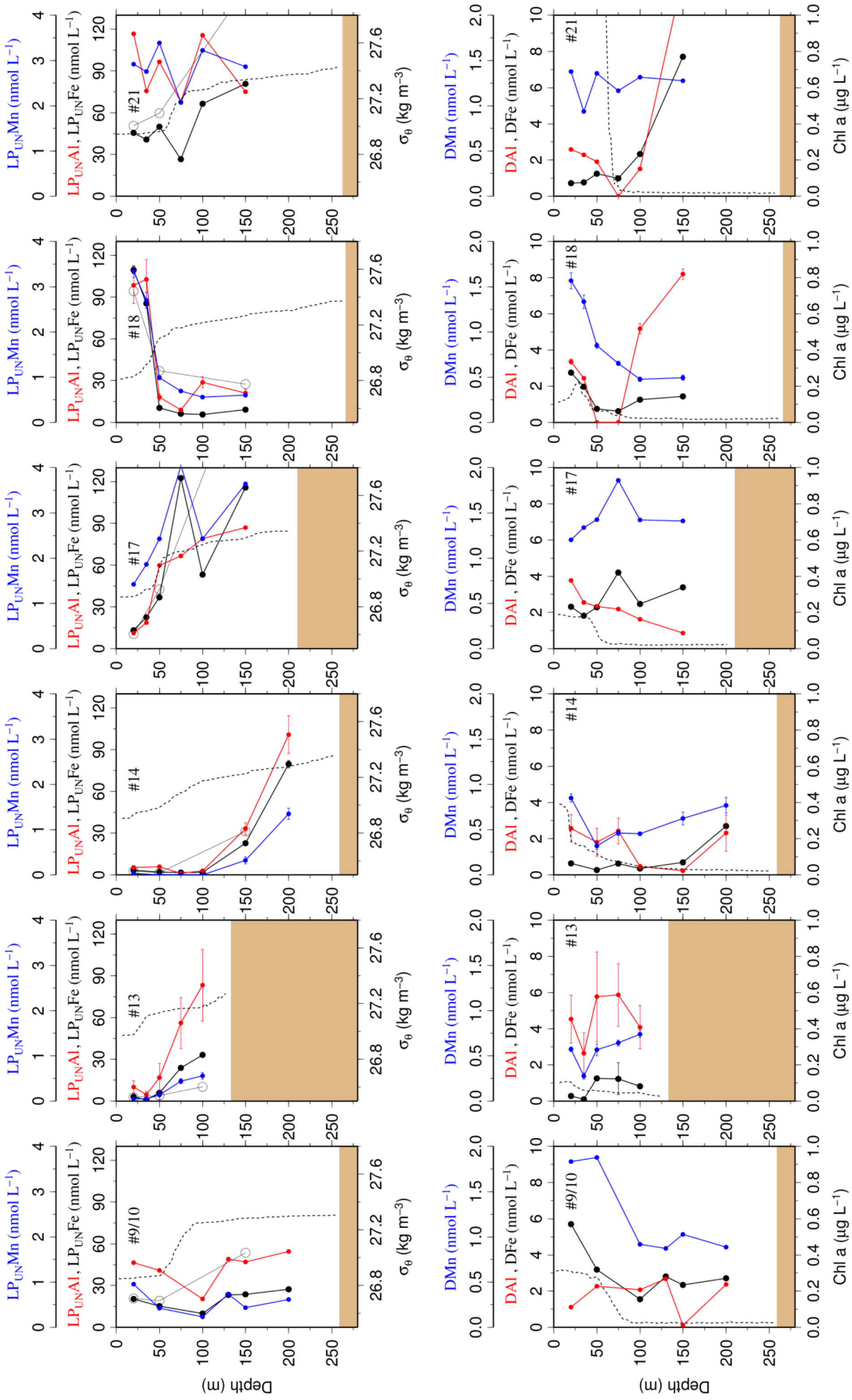

Biogeosciences Discuss., https://doi.org/10.5194/bg-2017-299
Manuscript under review for journal Biogeosciences
Discussion started: 28 July 2017

Figure 2: (Upper row) Distribution of particulates in unfiltered seawater samples ($LP_{Un}Fe$ in black), manganese ($LP_{Un}Mn$ in blue), and aluminium ($LP_{Un}Al$ in red) in the water column of stations located on the island shelf (125 m – 270 m water depth). The particulate Fe (PFe) fraction retrieved by SAPS is illustrated with open black circles and corresponds to the concentration labels of $LP_{Un}Fe$. Concentrations above 120 nmol L^{-1} are listed in Table 1 and 2. Error bars represent the standard deviation of the analysis. Density sigma-theta (σ_θ) in kg m^{-3} is illustrated by the black dashed line. (Lower row) Dissolved iron (DFe), manganese (DMn), and aluminium (DAl) are represented by the same colour code as above. Dashed lines illustrate Chlorophyll a (Chl a) content of the water column recorded by the CTD fluorometer.

Biogeosciences Discuss., https://doi.org/10.5194/bg-2017-299
Manuscript under review for journal Biogeosciences
Discussion started: 28 July 2017

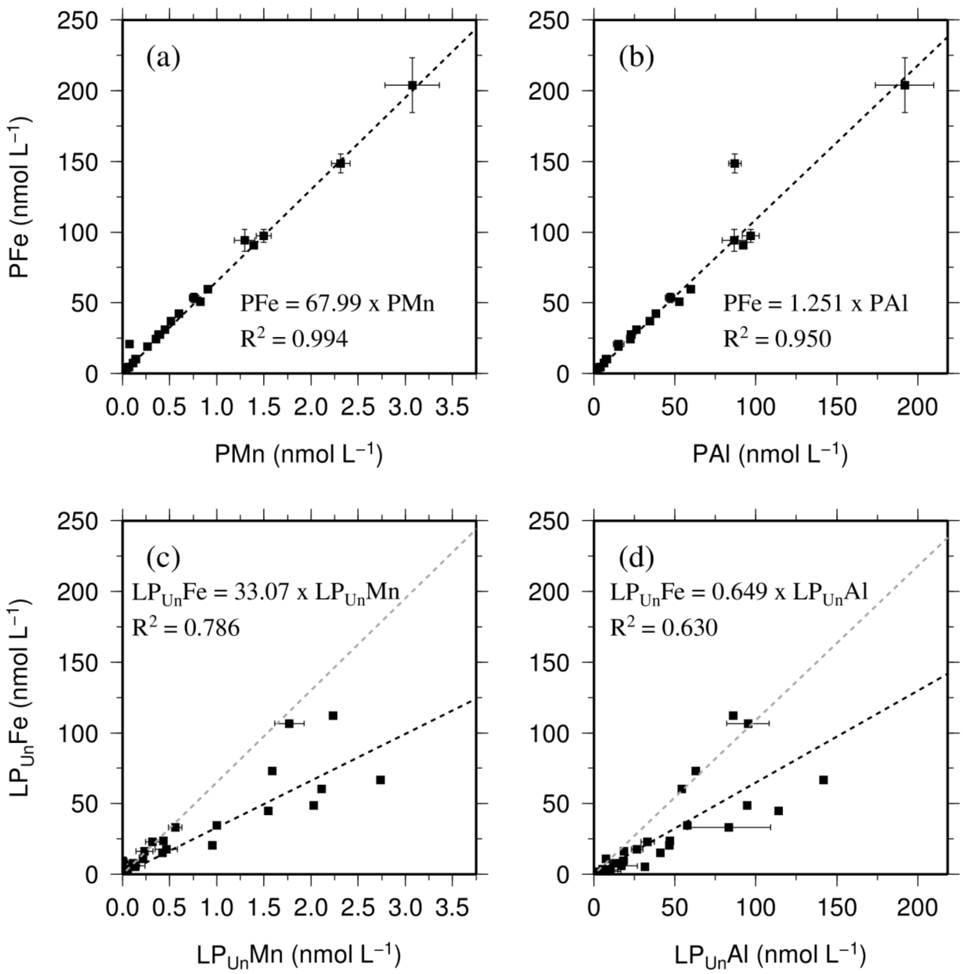

837

838 **Figure 3:** Relationship of the entire data set for the particulate fraction of Fe, Mn, and Al in
839 particulates (P) retrieved using SAPS ((a) and (b)) and the leachable particulate fraction
840 (LP_{UN}) estimated from unfiltered and dissolved seawater samples collected using OTE bottles
841 ((c) and (d)). Error bars represent the standard deviation of the analysis. The linear regression
842 of each relationship is illustrated by a dashed black line, the formula, and the R^2. The grey
843 dashed line in c. and d. represents the linear relationship of particulate trace meals (P) shown
844 in (a) and (b).

Biogeosciences Discuss., https://doi.org/10.5194/bg-2017-299
Manuscript under review for journal Biogeosciences
Discussion started: 28 July 2017

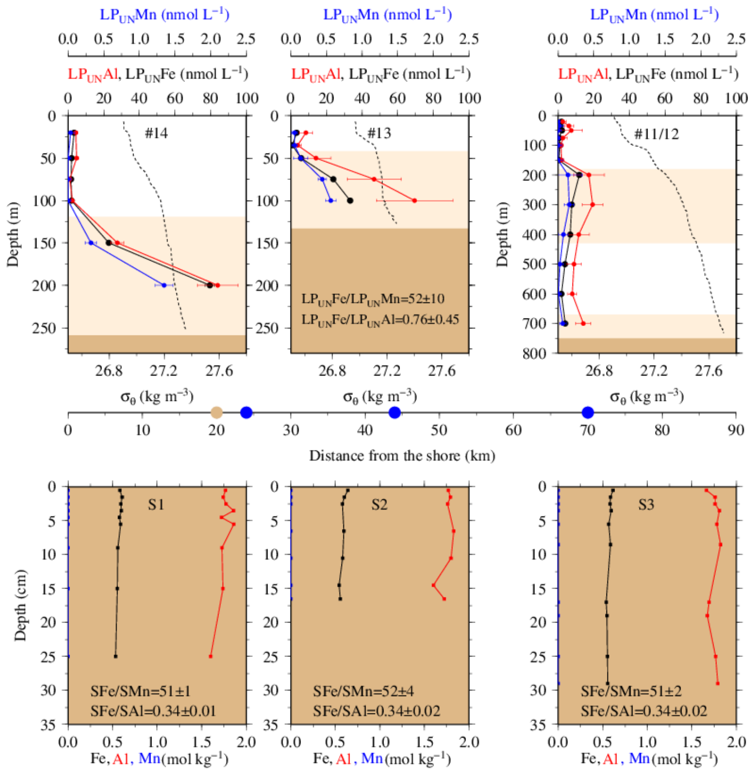

Figure 4: (Upper row) From left to right, concentrations of leachable particulate iron ($LP_{Un}Fe$), aluminium ($LP_{Un}Al$), and manganese ($LP_{Un}Mn$) of unfiltered seawater samples for the two shelf stations #14, #13 and the shelf edge station #11/12 (Note different depth scaling). Error bars represent the standard deviation of the analysis. Water density (sigma-theta (σ_θ)) is shown by the dashed black line. Brown areas represent sediments and pink areas the zone of resuspended sediment particles in the water column. Diagram 14 (left) contains the average $LP_{Un}Fe/LP_{Un}Al$ and $LP_{Un}Fe/LP_{Un}Mn$ ratio of particles in seawater samples collected within the pink layers. (Lower row) Diagram S1, S2 and, S3 displays the Fe, Mn, and Al content in the three sediment cores. Shown are average SFe/SAl and SFe/SMn ratios (mol/mol) of particles from the surface layer for station S1, S2, and S3. Dots on the distance scaling in the middle represent the distance of each water column station (blue) and sediment core (brown) station to the nearest shore.

Biogeosciences Discuss., https://doi.org/10.5194/bg-2017-299
Manuscript under review for journal Biogeosciences
Discussion started: 28 July 2017

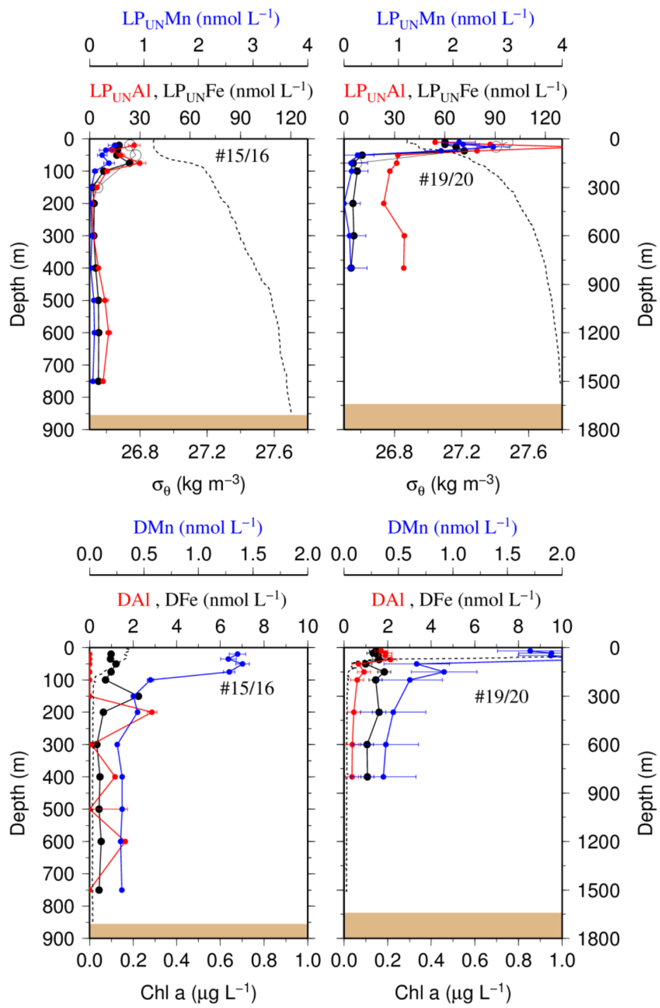

Figure 5: (Upper row) Distribution of leachable particulate manganese ($LP_{Un}Mn$ in blue), iron ($LP_{Un}Fe$ in black), and aluminium ($LP_{Un}Al$ in red) concentrations in the water column of the two other stations located on the island shelf edge (> 700 m water depth). The particulate Fe (PFe) is illustrated by black circles and corresponds to the concentration labels of $LP_{Un}Fe$. Error bars represent the standard deviation of the analysis. Sigma-theta (σ_θ) is illustrated by the black dashed line. (Lower row) Dissolved manganese (DMn), iron (DFe), and aluminium (DAl) are represented by the same colour code as for the upper row. Dashed line illustrates the Chl a content of the water column recorded by the CTD mounted fluorometer.

Biogeosciences Discuss., https://doi.org/10.5194/bg-2017-299
Manuscript under review for journal Biogeosciences
Discussion started: 28 July 2017

Biogeosciences Discussions

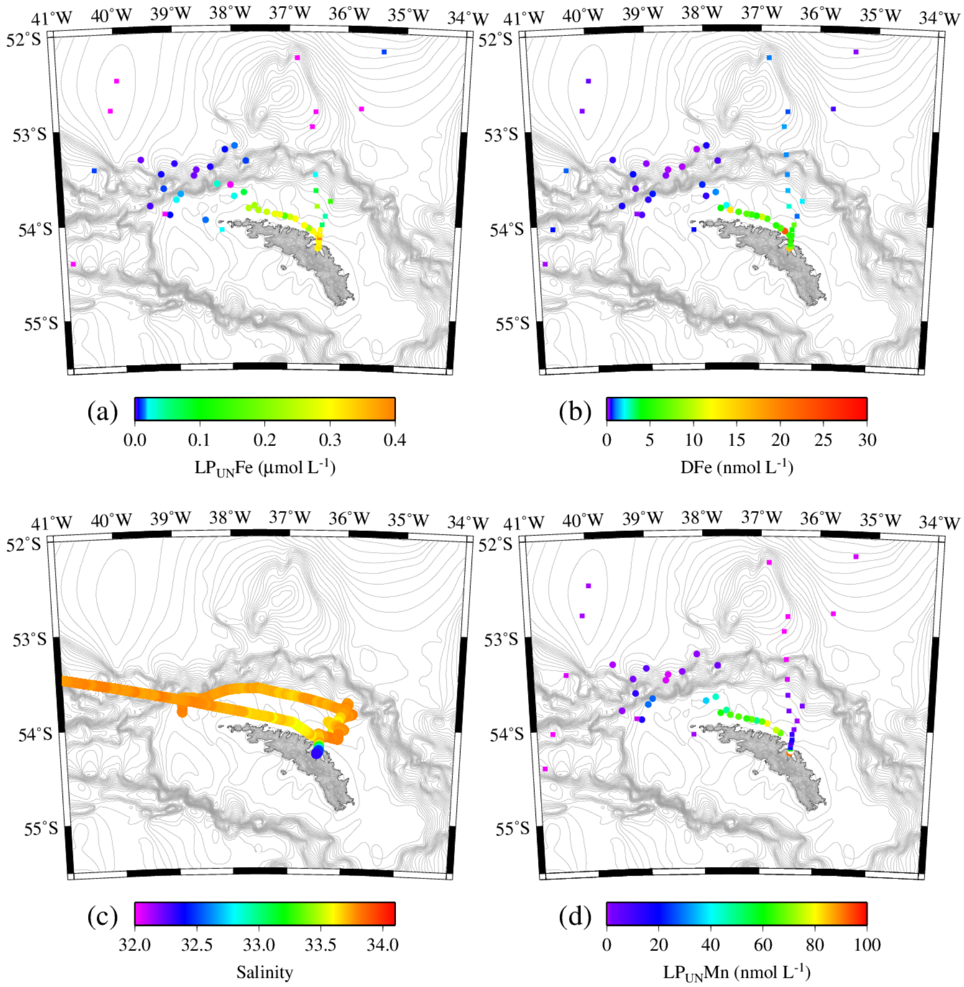

Figure 6: Concentrations of leachable particulate Fe ($LP_{UN}Fe$) of unfiltered seawater samples (a), dissolved Fe (DFe) (b), Salinity (c) and leachable particulate Mn ($LP_{UN}Mn$) in unfiltered seawater samples (d) in surface waters collected during JR247 (circles) and JR274 (squares) around South Georgia. Isobath are represented by grey lines (GEBCO – Gridded Bathymetry Data).

Biogeosciences Discuss., https://doi.org/10.5194/bg-2017-299
Manuscript under review for journal Biogeosciences
Discussion started: 28 July 2017

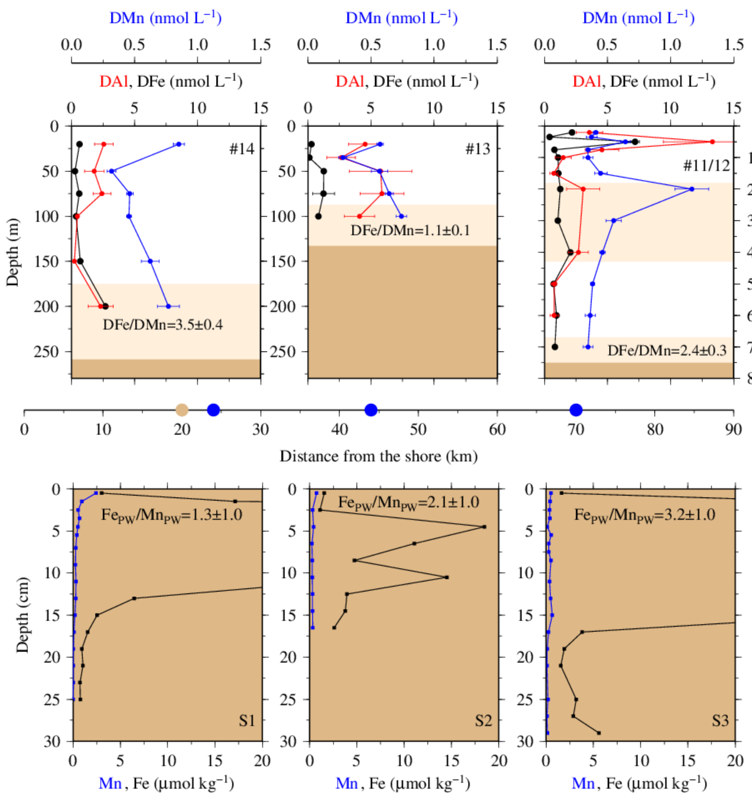

Figure 7: (Upper row) From left to right, concentrations of dissolved iron (DFe), aluminium (DAl), and manganese (DMn) for the two shelf stations (#14, #13) and the shelf edge station (#11/12). Note different depth scaling. Error bars represent the standard deviation of the analysis. Pink areas represent the zone of resuspended sediments in the water column. The DFe/DMn ratios of the seawaters collected within the pink zone is indicated. (Lower row) Diagram S1, S2 and, S3 displays the Fe (black), and Mn (blue) content in pore waters of the three sediment cores. Values off-axis can be found in Table 3. Shown are average Fe_{PW}/Mn_{PW} ratios (mol/mol) of top surface layer (1 cm) for station S1, S2, and S3. Dots on the distance scaling in the middle represent the distance of each water column station (blue) and sediment core (brown) station to the nearest shore.

Biogeosciences Discuss., https://doi.org/10.5194/bg-2017-299
Manuscript under review for journal Biogeosciences
Discussion started: 28 July 2017

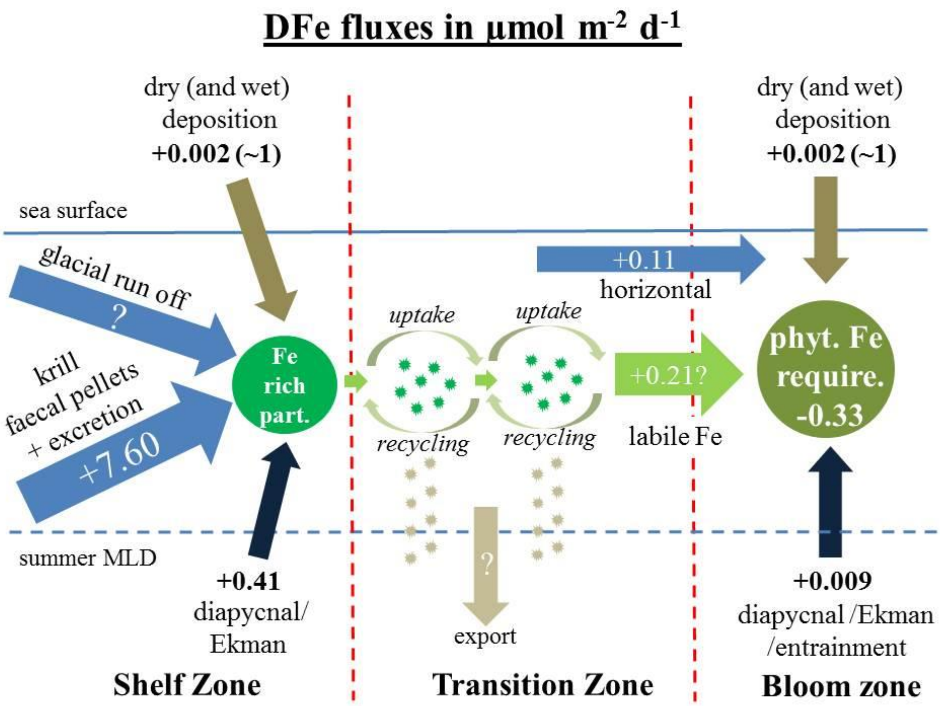

Figure 8: Sketch of DFe fluxes on the shelf, in the transition zone and in the downstream blooming region seprated by the red dashed lines. (left sketch) describes the dissolved Fe fluxes on the shelf that together generate Fe rich biogenic and lithogenic particles (dark green). These are transferred offshore (light green arrows) following the ACC to open ocean sites (sketch in the middle). Iron enriched particles (dark green suns) in the transition zone are recycled and supplement DFe requirements of the phytoplankton community in the transition zone. During each cycle of recycling and uptake an unknown Fe fraction is lost by vertical export. (right sketch) describes the dissolved Fe fluxes in the blooming zone.